Research Paper

A multidisciplinary study of an exceptional prehistoric waste dump in the mountainous inland of Calabria (Italy): Implications for reconstructions of prehistoric land use and vegetation in Southern Italy

Jan Sevink[1] , Wieke de Neef[2], Mauro A Di Vito[3],
Ilenia Arienzo[3], Peter AJ Attema[4], Emiel E van Loon[1],
Burkhart Ullrich[5], Michael den Haan[1], Francesca Ippolito[4] and
Nikolaas Noorda[4]

Abstract

The mountainous inland of northern Calabria (Southern Italy) is known for its sparse prehistoric human occupation. Nevertheless, a thorough multidisciplinary approach of field walking, geophysical survey and invasive research led to the discovery of a major archaeological archive. This archive concerns a rich multi-phased dump, spanning about 3000 years (Late Neolithic to Late Imperial Roman Age) and holding two Somma-Vesuvius tephra. Of these, the younger is a distinct layer of juvenile tephra from the Pompeii eruption, while the older concerns reworked tephra from the Bronze Age AP2 eruption (ca. 1700 cal. yr BP). The large dump contains abundant ceramics, faunal remains and charcoal, and most probably originated through long-continued deposition of waste in a former gully like system of depressions. This resulted in an inversed, mound-like relief, whose anthropogenic origin had not been recognized in earlier research. The tephras were found to be important markers that support the reconstruction of the occupational history of the site. The sequence of occupational phases is very similar to that observed in a recent palaeoecological study from nearby situated former lakes (Lago Forano/Fontana Manca). This suggests that this sequence reflects the more regional occupational history of Calabria, which goes back to ca. 3000 BC. Attention is paid to the potential link between this history and Holocene climatic phases, for which no indication was found. The history deviates strongly from histories deduced from the few, but major palaeorecords elsewhere in the inlands of Southern Italy (Lago Grande di Monticchio and Lago Trifoglietti). We conclude that major regional variation occurred in prehistoric land use and its impacts on the vegetation cover of Southern Italy, and studies of additional palaeoarchives are needed to unravel this complex history. Finally, shortcomings of archaeological predictive models are discussed and the advantages of truly integrated multidisciplinary research.

Introduction

Modern landscape archaeological studies generally involve a combination of field walking, geophysical surveys and invasive research (corings and pits). A typical example is the project Rural Life in Protohistoric Italy (RLP) in the Raganello Basin (Calabria, Italy), executed by the University of Groningen (see Armstrong and Van Leusen, 2012; De Neef, 2016; Sevink et al., 2016; Van Leusen et al., 2014). Within its scope, particular attention was paid to the northern part of the Raganello catchment (see Figure 1), a mountainous inland area with a low density of archaeological sites and with a geology dominated by Miocene clastic rocks.

In this area, site RB073 is situated on a slope that based on earlier research was assumed to be severely eroded and

nearly devoid of archaeological remains (Feiken, 2014). However, corings at this site showed the presence of a thick sequence of anthropogenic layers with abundant

[1]Institute for Biodiversity and Ecosystem Dynamics (IBED), The Netherlands
[2]Department of Archaeology, Ghent University, Belgium
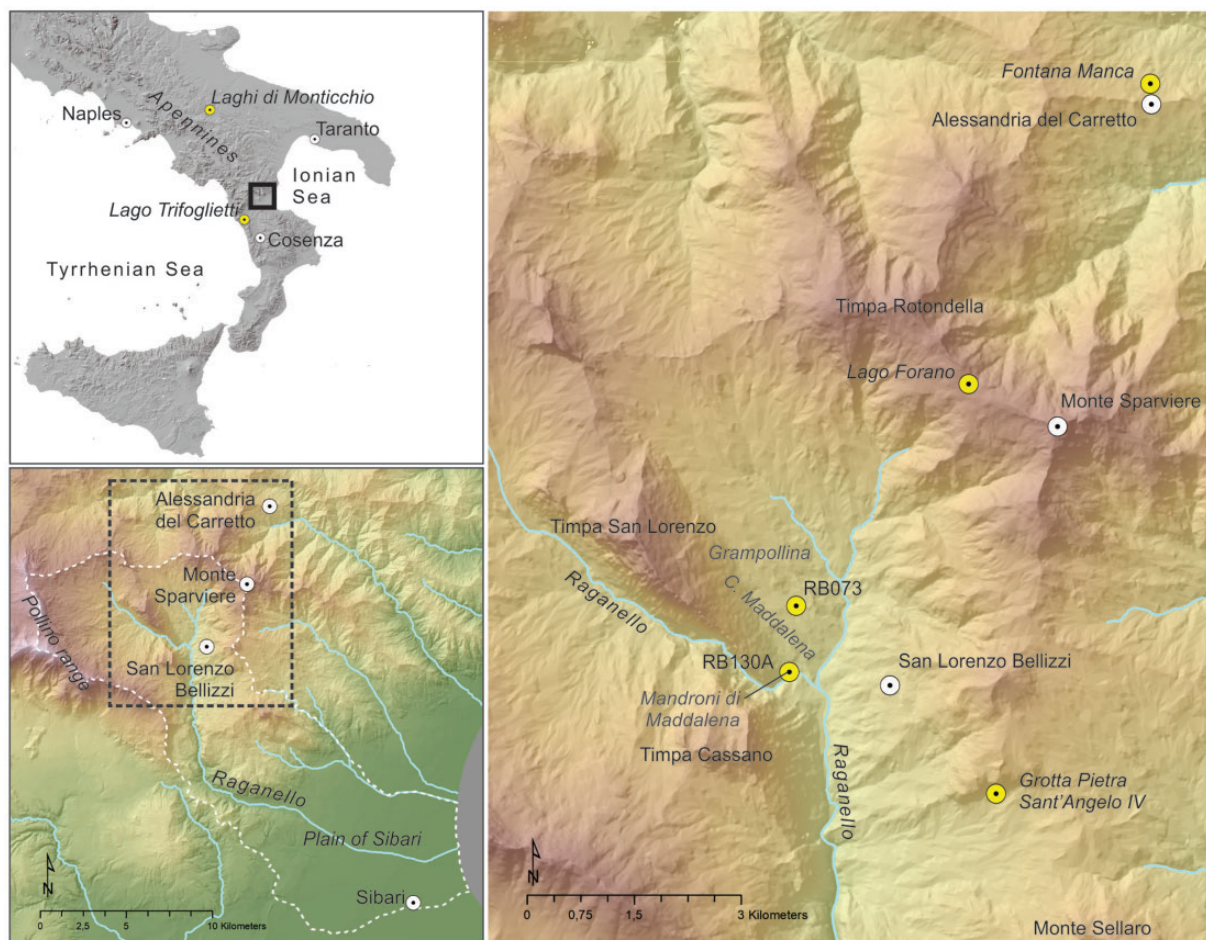[3]Istituto Nazionale di Geofisica e Vulcanologia (INGV), Italy
[4]Groningen Institute of Archaeology, The Netherlands
[5]Eastern Atlas GmbH & Co. KG, Germany

Corresponding author:
Jan Sevink, Institute for Biodiversity and Ecosystem Dynamics (IBED), P.
O. Box 94240, 1090 GE Amsterdam, The Netherlands.
Email: j.sevink@uva.nl

Figure 1. Location of the area of study and site RB073.

charcoal, fragments of ceramics and bones, as well as with a layer of tephra that based on ^{14}C datings originates from the Vesuvian Pompeii eruption in 79 AD (De Neef, 2016; De Neef et al., 2017; Sevink et al., 2016). This complex sequence of layers was further studied in two small pits (De Neef, 2016) that reached down to about 2 m depth, but did not yet reach the underlying in-situ soil or regolith.

Initially, it was assumed by Sevink et al. (2016) that the complex sequence represented a mound-like accumulation of Bronze Age and later anthropogenic layers over a protruding slope that previously was more regular. A subsequent magnetic gradiometry survey (De Neef, 2016) revealed a pattern that suggested the occurrence of a complex, branching gully like system, filled in with anthropogenic materials. However, streams that might have cut such gullies were not observed and, alternatively, the observed pattern might be linked to a complex bedrock geology.

To establish the nature of the geomagnetic feature – bedrock geology or gully like system–an extensive coring programme was executed. The results from these corings and the magnetic gradiometry survey were statistically analysed to establish the relations between the signal and the thickness of the anthropogenic layers. Magnetic properties of the various materials encountered at this site were assessed to provide an explanation for the empirical relations found. Based on this analysis a 3-D model of the feature was constructed.

The complex of anthropogenic layers encountered in the corings comprised several dark, humic layers and locally was up to 4 m thick. It contained abundant ceramic, bone and charcoal fragments. Several corings or parts thereof were studied in more detail, paying attention to the identification of the various anthropogenic materials, ^{14}C dating of charcoal fragments from deeper strata, and the occurrence and provenance of tephra.

In this paper, results are presented from this truly multi-disciplinary study of the exceptional multi-phased site. We employed a range of techniques and methods that primarily served to identify the dimensions, composition and age of the anthropogenic layers. Results on the first are presented in sections 'Materials: Macroscopic characteristics' to 'Cores and pits: Fill composition'; while in section 'Dating: [14]C ages, ceramics and tephra', we describe the dating results for the various materials (tephra, charcoal and pottery). In the discussion, we first focus on the morphology of the gully like system (section 'Morphology of the regolith surface') and the identification of the tephra (section 'Tephra'), which play an important role in the identification and dating of the various phases distinguished in the fill. The latter is described in an extended section ('Age of the "anthropogenic layers": tephra, ^{14}C dating, ceramics and phases'). In section 'Gully like system and fill: genesis', the genesis and age of both the gully like system and its fill are discussed in a more general context. Our results in terms

of the occupational history and archaeological record are discussed in a regional context in section 'Correlation of phases with relevant archaeological, vegetational and palaeoclimatic records'. This section is focused on the correlation of phases with other relevant archaeological, vegetational and palaeoclimatic records.

In section 'General discussion and conclusion', we discuss the main results of our study, particularly the occurrence of tephras and their use as marker bed, and the considerable spatial and temporal variation in prehistoric land use and vegetation cover at the scale of Southern Italy. Finally, we pay attention to the importance of a combined approach – field walking, geophysical survey and invasive research – in landscape archaeological studies and to some limitations of archaeological predictive modelling.

Background information

The northern Raganello catchment consists of a lower area with Miocene clastic rocks – the Contrada Maddalena – confined between two large ranges, the limestone-dominated Timpa di San Lorenzo/Timpa di Cassano range and the Monte Sparviere/Timpone della Rotondella/Monte Sellaro range, which has a more varied geology (Ghezzi, 1973; Giannini et al., 1963). This geological structure is clearly visible in Figure 2. The Miocene clastic rocks hold variable amounts of calcium carbonates (up to marls) and are mostly fine-grained and only slightly metamorphosed (predominantly shale and phyllite, and rare schist). They are unstable and sensitive to erosion and mass movements. In places, huge boulders and blocks of limestone debris occur, originating from the adjacent limestone ranges, as well as limestone debris cones that formed at the foot of these ranges. These limestone-derived deposits protect the underlying Miocene clastic rocks against erosion and often stand out as ridges (Feiken, 2014; Sevink et al., 2016). The Miocene rocks are dense, fine textured and of low permeability, giving rise to water stagnation and surficial runoff upon continued rainfall (see Feiken, 2014). In the limestone debris, local aquifers may build up, leading to small perennial streams, which eventually also are fed by springs at the mountain front. Streams, originating in the clastic rock-dominated areas, are truly scarce and run intermittently.

The area of study, with site RB073, is a field situated on a fairly gentle SSE-oriented slope with a small promontory hillock, beneath a larger ridge capped by large limestone blocks that originate from the nearby Timpa di San Lorenzo range. The dominant local rock types are marl and shale/phyllite, with possibly some bands of limestone and iron-rich sandstone. The latter is suggested by the occurrence of large fragments of such rocks at the surface (Sevink et al., 2016). An agricultural terrace borders the lower part of the field. This stonewall terrace is about 1.5 m high. The topography of the area can be seen in Figure 3, which additionally shows the location of corings on which the cross section was based, presented by Sevink et al. (2016).

The archaeological occupation of the upland valley is best known from the limestone-based zones including bluffs, caves and debris slopes. Evidence from the Middle Neolithic to the Late Bronze Age was recorded at the south-facing debris slope below the Timpa Sant'Angelo, while
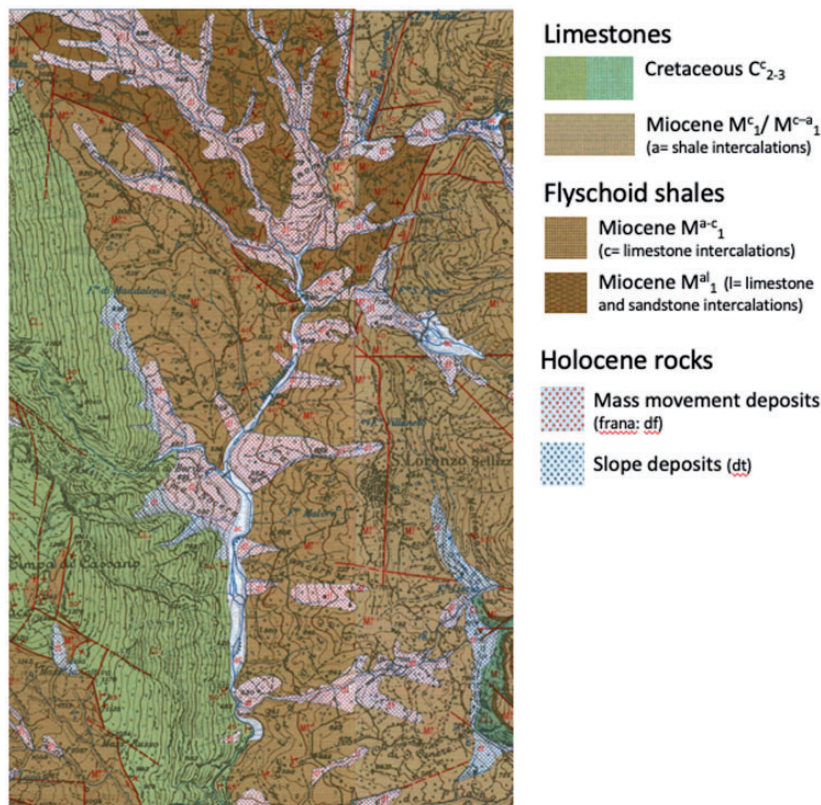
Figure 2. Summary geological map of the Contrada Maddalena and adjacent ranges showing the major formations. Based on the 1:25,000 geological maps, sheets 221-1-so/se. For details on the legend units, see the legends to these maps (https://www.sciamlab.com/opendatahub/dataset/regcal_carta-geologicaraster1-25,000).
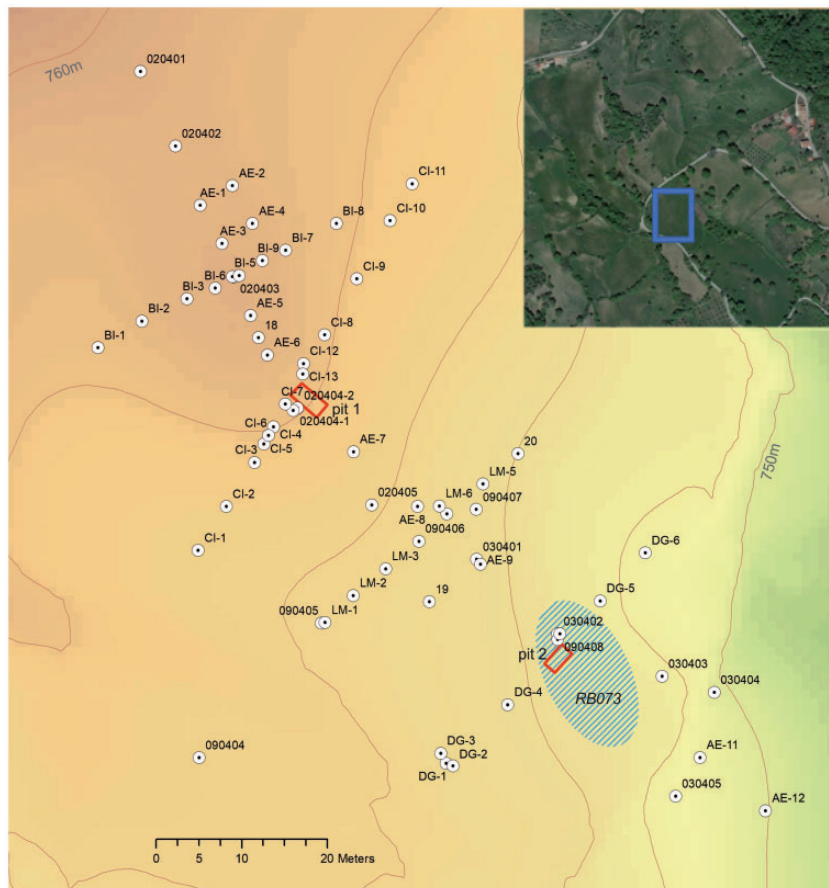
Figure 3. Area of study with location of corings and pits (red rectangles). Corings 2015: transects AE-BI-CI-LM-DG. All other corings are from 2013. Contour line interval is 2 m.

ongoing excavations in the nearby Grotta Pietra Sant'Angelo IV by the Universities of Bari and Molise brought to light a Chalcolithic burial and other traces of prehistoric activity (Larocca et al., 2019). A test pit excavated at site RB130a on the debris slope of Mandroni di Maddalena, near the upper canyon of the Raganello river, revealed three ^{14}C-dated Middle Bronze Age occupation levels. The osteological record from these phases indicates that the occupants of this site practised a mix of (agro-) pastoralism and hunting (De Neef, 2016). The results for the test pit revived the question of whether sites in this upland valley are seasonal camps or year-round settlements, but it was concluded that more extensive excavations are needed to address this issue. On the basis of ceramic fabrics, Ippolito (2016) dated the majority of surface sites in the limestone areas to the Middle and Recent Bronze Age (ca. 1700–1350 BC), after which the uplands appear to have been abandoned in favour of the lowlands surrounding the coastal plain of Sibari.

The archaeology of the open undulating landscape of the Contrada Maddalena is more difficult to interpret than that of the limestone zones. Between 2006 and 2010, the Groningen Institute of Archaeology mapped 20 archaeological sites during intensive systematic field walking surveys. All of these are small scatters of handmade Metal Age pottery (2nd millennium BC), except for one Hellenistic/Roman scatter (site RB176). Stray finds of lithic tools in local quartzitic sandstone indicate Palaeolithic presence in the Grampollina area, but discrete Stone Age activity foci have

so far not been identified (Van Leusen and De Neef, 2018). The poor preservation status of the Metal Age ceramics hinders our understanding of the functionality and temporality of the surface pottery scatters in the Contrada Maddalena.

Representative examples of sites from the Metal Age were investigated in detail during the RLP project (2010–2016). The preservation and detection of Metal Age traces in the Contrada Maddalena were found to be strongly related to post-depositional processes. This led Feiken (2014) to develop the predictive Caleros model, which attempts to assess the bias in the archaeological record largely by means of a complex soil erosion model. The best-preserved occupation traces indeed occurred on debris slopes near limestone bluffs where archaeological deposits are sealed through episodic rock fall, whereas the open-air sites in the erosive undulating sloping landscape tended to be related to secondary or tertiary deposits (De Neef et al., 2019). Site RB073 belongs to this second type of deposits. Its preliminary study in the form of two test pits (De Neef, 2016) and coring transects (Sevink et al., 2016) already indicated that the occupation of the open undulating land in the Contrada Maddalena started earlier than previously thought, probably coeval with the limestone-based sites, and that locations like these were in repeated use over long periods of time. It was in these pits and corings that the first tephra layer was encountered, identified as juvenile tephra from the Pompei event (Sevink et al., 2016).

Major middle- to late-Holocene eruptions that left significant traces in this part of the Central Mediterranean

area have been described by Zanchetta et al. (2011). They include the Astroni-Agnano MS eruptions (Campi Flegrei: 4240 ± 90-4680 ± 100 cal. yr BP), the Avellino (or AV) eruption (Somma-Vesuvius: 3810 ± 60 cal. yr BP) and the Pompeii eruption (Somma-Vesuvius AD 79). Ages reported in more recent studies may somewhat deviate, but the overall picture of these major eruptions is identical. Recently, tephra from several minor eruptions has been reported in marine cores from the Central Mediterranean, nearly always in the form of cryptotephra (Crocitti et al., 2019; Di Donato et al., 2019; Insinga et al., 2020; Zanchetta et al., 2019). Particularly relevant for our research are the studies by Zanchetta et al. (2019) and Insinga et al. (2020). They describe that other eruptions potentially relevant for Calabria, include the Somma-Vesuvius AP1-6 events and the Etna Sicani event. The first seem incorrectly dated by Insinga et al. (2020), given the datings by Passariello et al. (2009) and Di Vito et al. (2019), which place the AP2 eruption at ca. 1700 cal. BC or slightly later and found the other AP eruptions (AP3-6) to be considerably younger. The Sicani event produced the FL tephra that according to Zanchetta et al. (2019) dates from ca. 3.3 cal. ka BP. However, Insinga et al. (2020) describe the FL tephra as erupted in two phases, of which the earliest (3625 ± 96 cal. yr BP) produced benmoreitic dark grey porphyritic scoria, and the younger (3361 ± 76 cal. yr BP) mugearitic/tephriphonolitic dark dense scoria and greyish pumice, with loose crystals of olivine, pyroxene and brown mica.

In distal positions, both the AP1-6 and the FL tephra occur as cryptotephra. They were found in a marine core from the Gulf of Taranto (Insinga et al., 2020), but in terrestrial sequences from this part of mainland Southern Italy they seem to be very rare. Tephra layers found in northern Calabria and adjacent parts of Campania and Basilicata include the distinct layer of juvenile tephra from the Pompei eruption, described in the 'Introduction' (Sevink et al., 2016), and a thin layer of juvenile AP2 tephra at Alessandria del Carretto (Sevink et al., 2019). The latter tephra was identified by its mineralogy, $^{87}Sr/^{86}Sr$ isotopic composition of feldspar and pyroxene crystals, and radiocarbon dating of the peat sequence in which it was intercalated. Finally, Boenzi et al. (2008) described two tephra layers in their study of the Basento River Basin and identified these as Avellino and AP3 tephra, but their attribution seems to be based on a few radiocarbon datings only and therefore is uncertain (see discussion in Sevink et al., 2019). Thus far, the Etna LF-tephra has not been reported for mainland deposits from Southern Italy. The various relevant tephra described in the literature are indicated in Figure 10.

Methods

Following on systematic field walking to record the surficial occurrence and distribution of artefacts, a preliminary geomagnetic survey (GMS-1) was performed and soils were cored along a transect. The results were reported by Feiken (2014), De Neef (2016) and Sevink et al. (2016). Subsequently, De Neef and Ullrich performed a detailed magnetic gradiometry survey (GMS-2) of the field in which site RB073 is located, using a mobile LEA-MAX system with six Foerster FEREX CON650 fluxgate gradiometer probes arranged at 50-cm intervals. While the cart is moved along parallel profiles at walking speed, the

individual sensors measure the vertical component of the Earth's magnetic field (the gradient) with a sensitivity of 0.1 nT (nanoTesla). The difference between the readings in each set of sensors is used to map local variations at an in-line point resolution of 5 cm. The data were positioned using a differential GPS set up with a rover mounted on the cart and a base station further away, plus an odometer in one of the cart's wheels. The relative accuracy of the dGPS readings was 2 cm. Data processing included decoding, statistical drift correction and normalization, and gridding using a Kriging routine with a search radius of 70 cm. The gridded data are a 2D representation of spatial patterning in near-surface variations in the vertical component of the Earth's magnetic field at a resolution of 25×25 cm^2.

The detectability of magnetically enhanced objects or deposits depends on a range of parameters including, inter alia, the contrast in magnetic susceptibility between a feature and the surrounding soil, depth of burial, volume and dimensions of features, and post-depositional processes. In archaeological prospection, the spatial patterning in these contrasts and the strength of the recorded parameter, expressed by the amplitude of the signal, are used to interpret such data in terms of archaeological relevance. Here, we used a representation at ± 5 nT (see Figure 4a).

An Edelman corer with a diameter of 7 cm was used for coring several transects (Figure 3), sampling each 10 cm in a more limited number of corings (volume of ca. 70 cm^3). Coring positions (x/y/z coordinates) were established using a total station. Soil materials encountered were described in the field using the FAO Guidelines for soil description (Jahn et al., 2006). Amounts of fragments of ceramics, bone and charcoal were semi-quantitatively estimated, as well as the amount and nature of gravel-size and coarser rock fragments. Corings were continued till the bedrock or large rock fragments prohibited further coring. The identification of the transition from anthropogenic material to in-situ material (more or less truncated soil, regolith or bedrock) was primarily based on the presence or absence of anthropogenic materials (ceramics, bone, and charcoal). Other characteristics used include hydromorphic features (mottling), consistence and texture. These allow for distinction between a truncated soil or regolith, and later anthropogenic material (the 'fill', see below).

In most instances where stones were encountered and prevented further coring, repeating the coring very close to the original location (at less than 50 cm distance) allowed for its further extension. This evidenced that most coarse rock fragments were not bedrock, but loose fragments. However, this did not apply to all corings and in these rare cases doubts remain about the 'true depth' at which in-situ (autochthonic) material occurs below the 'fill', defining this 'fill' as the total of layers of anthropogenic (allochtonic) material. In most cases, we found slightly weathered rock (regolith) immediately below the fill, rapidly grading into fresh bedrock. Buried soil horizons (i.e. remains of the original prefill soil), if present at all, were weakly developed, having the characteristics of a B/Cg horizon. For convenience, we define the depth to in-situ material as the 'depth to regolith'.

Statistical correlations between the magnetometry readings (GMS-2) and 'depth to regolith' were analysed using all available coring data. The basic area (basic pixel) for individual GMS measurements was 25×25 cm^2, but evidently the geomagnetic signal for fill depths as encountered in the
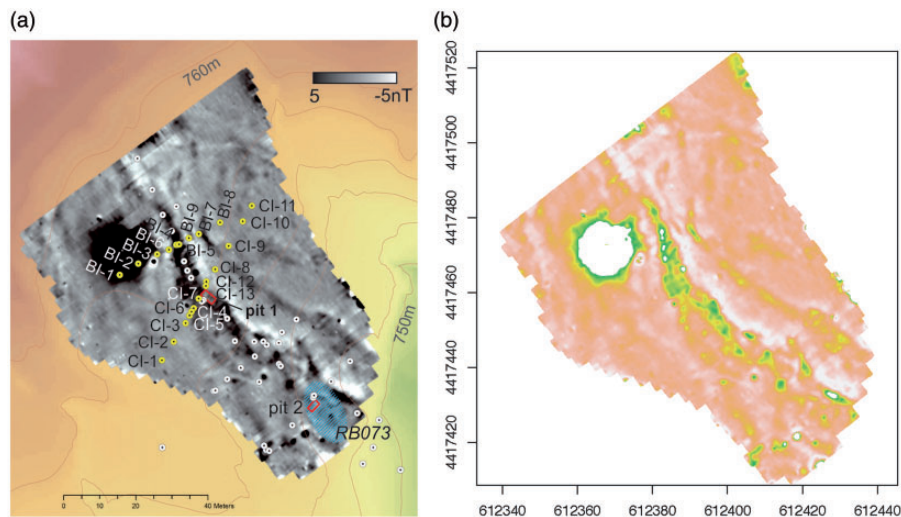
Figure 4. (a) Magnetic gradiometry map of the area of study. Black dot at Bl-1/2 is because of the presence of a small electric power station interfering in the signal. Small dots indicate location of corings. (b) Derived map showing depth to regolith in centimetres, based on observed optimal statistical relation between signal strength and 'true depth to regolith'.

area of study is dependent on a larger volume of material and at the scale of a basic pixel may vary strongly due to very locally present 'aberrant' materials (e.g. minute iron fragments in manure). To study the impact of pixel size and eliminate very local signal peaks, we analysed the statistical relation for a range of larger pixel sizes, defining these as the diameter of the pixel for which the mean signal strength is calculated. Functions such as the weighted mean value or a distance-to-centre related function might be used for obtaining the value to be used in the statistical approach, but we refrained from doing so and used spheres of different radii to establish at what radius correlations are optimal.

Given the uncertainty about the true depth to regolith, for the statistical analysis we used two data sets as follows:

1. Data on all corings, either 'depth to regolith' or maximum coring depth as limited by coarse sized, hard rock fragments;
2. Data on only those corings for which 'depth to regolith' could be reliably established, based on expert judgement of the macroscopic characteristics of the material during coring, being in-situ rock, regolith or more or less truncated soil. This data set is referred to as the 'true depth to regolith'.

The observed optimal statistical relation between 'depth to regolith' and pixel radius was used to construct a map showing the depth to regolith. Mean signal values for the optimal pixel size were calculated from the basic data, using a moving average.

For a selection of cores and core sections, samples (ca. 70 cm^3) were dispersed in water and wet sieved over a >63 um sieve. Residues were microscopically checked for the presence of ceramics, bones and charcoal, as well as the composition of the gravel and sand fractions. Materials recorded were charcoal, ceramics, bones, chert and rock fragments (fraction >2 mm), and volcanic tephra (in sand fraction). Fragments of ceramics were identified by De Neef and Ippolito, based on their expert knowledge of the ceramics encountered in Southern Italy (see e.g. Ippolito,

2016). Kuijper identified the animal remains (mostly bone fragments).

[14]C datings on charcoal samples were performed at CIO (Groningen) following on an ABA pretreatment. Samples from cores were obtained by hand-picking from sieve residues (see above) and from samples from the test pits. Values obtained were age calibrated using the OxCal4.3 software package (Bronk Ramsey, 2017) and the IntCal 13 calibration curve. Most samples were charcoal, but some were bone fragments from which collagen was extracted using the ABA-Longin chemical pretreatment (Longin, 1971).

Tephra was analysed to determine the chemical and isotopic compositions of the glass and mineral fractions to provide an independent time constraint. Chemical analyses of thin sections with tephra particles were performed at the HP-HT Laboratory of Experimental Volcanology and Geophysics of the Istituto Nazionale di Geofisica e Vulcanologia at Rome (Italy), using a Cameca SX50 electron microprobe equipped with five wavelength-dispersive spectrometers using 15 kV accelerating voltage, 15 nA beam current, 10 Am beam diameter and 20 s counting time. Analyses were performed on samples from the corings and pits at site RB073, as well as from the tephra layer encountered at Fontana Manca (Sevink et al., 2019). The latter tephra layer was identified as the AP2 tephra layer from the Somma-Vesuvius, dated as such on the basis of its mineralogy, Sr-isotopic ratio and ^{14}C datings.

Sr isotopic compositions were determined on separated minerals by Thermal Ionization Mass Spectrometry at the Istituto Nazionale di Geofisica e Vulcanologia at Napoli (Italy), using a ThermoFinnigan Triton TI multicollector mass spectrometer. Before chemical dissolution, ca. 0.1 g of feldspar and pyroxene crystals were ultrasonically cleaned in diluted hydrofluoric acid (7%) and then rinsed with MilliQ® water. Following leaching, the minerals were dissolved with high-purity HF-HNO3-HCl mixtures. Sr was separated from the matrix through conventional ion-exchange procedures, described in detail in Arienzo et al. (2013). The measured $^{87}Sr/^{86}Sr$ ratios were normalized for within-run isotopic fractionation to $^{86}Sr/^{88}Sr = 0.1194$. Sr

blanks were of the order of 0.2 ng during the period of chemical processing. During collection of isotopic data, replicate analyses of the NIST-SRM 987 (SrCO₃) international reference standard were performed to check for external reproducibility. The standard error with $N = 180$, that is, $2\sigma_{mean}$, was better than ± 0.000010 for Sr. The external reproducibility 2σ (where σ is the standard deviation of the standard results), that is, the mean measured value of $^{87}Sr/^{86}Sr$ for the NIST-SRM 987 standard, was 0.710204 ± 0.000019 (2σ, $N = 72$). The external reproducibility (2σ) is calculated according to Goldstein et al. (2003). Sr isotope ratios of the samples analysed, as well as those from the literature used for comparison, were normalized to the recommended values of NIST-SRM 987 ($^{87}Sr/^{86}Sr = 0.71025$) standard.

Results

Materials: Macroscopic characteristics

By far the dominant type of in-situ material encountered below the 'fill' was more or less weathered marl to shale/phyllite. Limestone and sandstone (including iron-rich varieties) were not encountered, but in the fill fragments of limestone and (lesser) sandstone were common. Moreover, a scatter of gravel to boulder-size angular fragments of these rock types was observed at the surface, while in the pits they were found as more or less distinct layers (see Figure 5a and b). Depth to 'in situ regolith' ranged from less than 50 cm to about 400 cm.

The results for the fill can be summarized as follows:

- The fill consisted of a series of anthropogenic layers of varied colour and textural composition, as was the case in the pits and corings reported by De Neef (2016) and Sevink et al. (2016). Particularly in deeper fills, dark layers were common. In soil description terms (FAO, 2006), these are A horizons because of their dark colour and slightly higher organic matter content, more specifically Au horizons (u = urban and other human-made materials), but in archaeological terms they most probably are occupational horizons and reflect periods of slope stability (see Figure 5a and b).
- The maximum number of A horizons encountered was at least 5, with the Pompeii tephra layer occurring in the second, commonly compound A horizon. However, in the majority of the corings and especially in thinner fills, a smaller number of A horizons were found or even no distinct A horizon at all.
- The fill exhibited a wide range in content of charcoal and fragments of ceramics and bones, and regularly held more than 5% ceramics and bones (by weight). Examples are given in the description of the individual cores (see Table 2). Sizes of fragments encountered in the corings were up to 5 cm. Original sizes may have been considerably larger as evidenced by their presence in the layers, exposed in the pits, as described by De Neef (2016).
- Some layers contained large boulder and stone size angular rock fragments, mainly of limestone, and some layers were nearly entirely composed of such fragments (see also Figure 5a and b).

- In a fairly large number of corings, the Somma-Vesuvius Pompeii tephra layer was found as a distinct, centimetres thick, loose fine sandy to silty tephra layer (see e.g. Figure 5a, layer US 6). Given its characteristics, notably its considerable inclination (20–30°), we conclude that this is a layer of juvenile tephra. In several deep corings at some depth below this Pompeii tephra layer, a layer holding some reworked tephra was encountered. This deeper layer was macroscopically identifiable by its colour and mineral composition. Corings in which the Pompeii tephra layer was observed are indicated with * in Figure 6.

## Depth to regolith and geomagnetic survey

The results from the magnetic gradiometry survey are presented in Figure 4a (see also De Neef, 2016). From the statistical analysis it appears that R^2 values of statistical relations are the highest for 'true depth to regolith' values in combination with pixels with a radius of 1.0 m. For that radius, the R^2 values for quadratic and linear regressions are nearly identical (0.47 vs 0.48). Figure 7 shows the 'true depth to regolith' versus signal for the optimal radius (1.0 m). The observed statistical relation between signal and radius (quadratic regression) has been used to translate the measured signal values over the radius concerned to a map of 'depth to regolith'. The results are presented in Figure 4b, together with the initial gradiometric map. In Figure 6, transects are presented based on the original coring data, also showing the occurrence of A horizons and tephra, and the location of the ^{14}C samples and their age (sections 1a and 2a).

Figure 7 shows that considerable variation occurs in the range of signal strength for relatively shallow depths that is, to about 2 m and seemingly is less variable for cores in which regolith is encountered at larger depths. For a full understanding of the causes of this variability, insight into the magnetic properties of the various anthropogenic layers that together and in varying proportions constitute the fill is essential. Data on these properties are shown in Figure 5a and pertain to the gridded magnetic susceptibility measurements on the pit sections by Armstrong using a Bartington MS3 with a point (F-) sensor at a resolution of 10 cm. Three readings were taken at each point and subsequently averaged (De Neef et al., 2017).

Cores and pits: Fill composition

Descriptions of the pits have already been published elsewhere (De Neef, 2016) and are summarized in Table 1. Cores and core sections studied in more detail are listed in Table 2. Cores BI5, AE7, CI7 and CI4 are from deep fills in the central depression and were particularly studied for the variation in texture and composition, the presence of tephra and possibilities for ^{14}C dating. Core DG3 is from a local, small pit-like depression, whose fill was extremely high in ceramic and bone fragments, as well as in charcoal.

In Table 2, semi-quantitative data on ceramics, bone, charcoal and other anthropogenic constituents are listed, as well as the results for identification of the ceramics and animal remains encountered (see also section 'Dating: ^{14}C ages, ceramics and tephra'). In addition, the presence of tephra, based on the recognition of volcanic components such as idiomorphic augite, diopsite, sanidine and dark
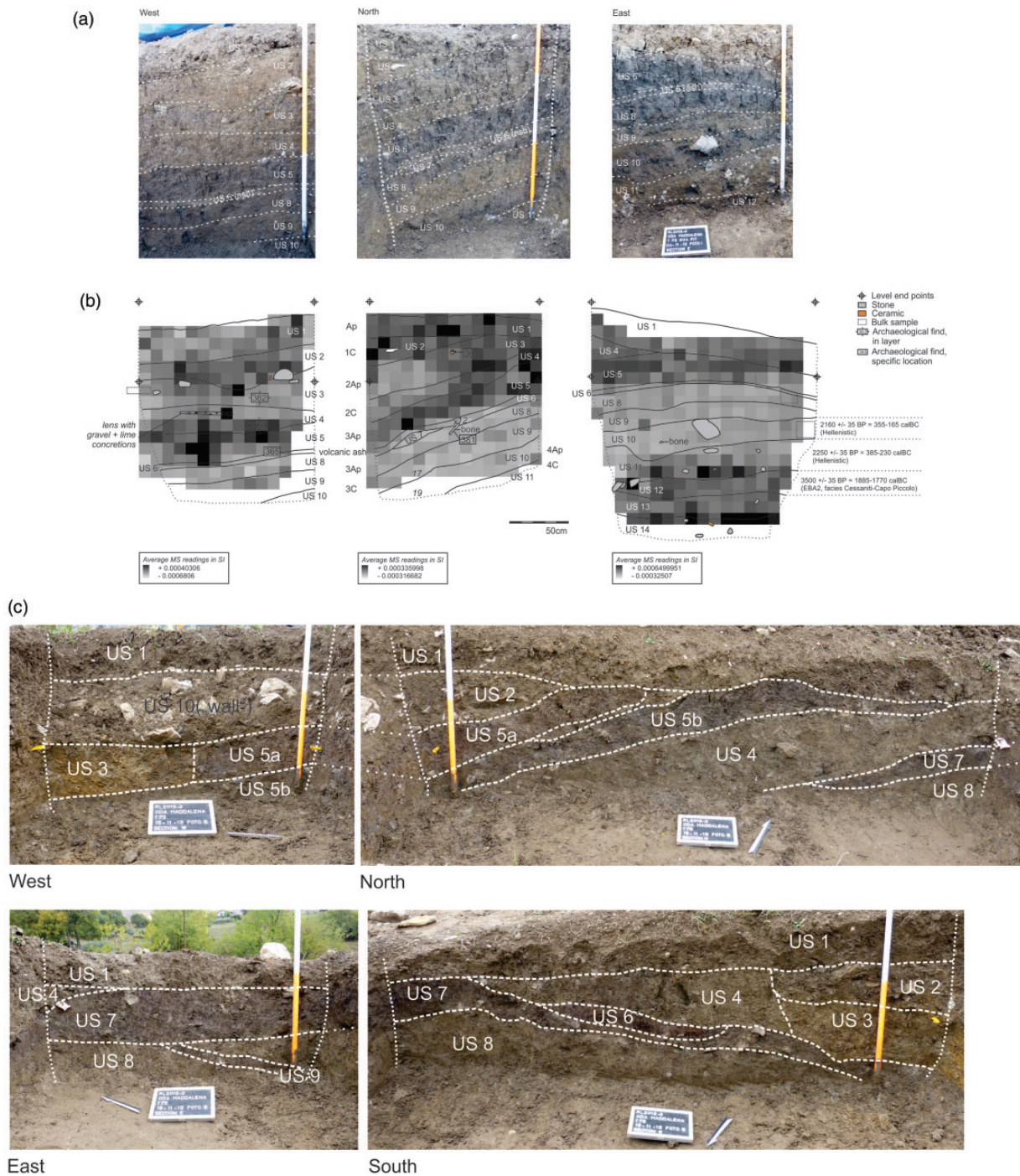
Figure 5. (a) Stratigraphy in pit 1, with inclined strata (see section North) holding the tephra layer from the Pompeii eruption (US6). (b) MS values in faces of pit 1. (c) Stratigraphy in pit 2. Numbers US 1, 2, 3 and so on refer to the field number given to layers distinguished in each individual pit (see also Table 1).

mica crystals, is indicated. Tephra from the Pompeii eruption could be identified by additional criteria such as by its very loose consistence, greyish colour and silty to fine sandy texture. Statements on the occurrence of tephra are based on microscopic study of the fractions >62 μm and thus do not concern eventually occurring finer (crypto)tephra.

Core BI5, which in the upper part contains the Pompeii tephra (around 100 cm depth, but not as a distinct individual layer), has three distinct buried A horizons, of which the lowest occurs between 260 and 270 cm, where it is covered by at least 40 cm material with abundant charcoal and ceramics. Tephra is present above this layer and is absent below. The composition of the material >63 um is rather constant, but in the deepest part of the coring the gravel fraction strongly increases. Regolith is encountered at 320 cm depth.
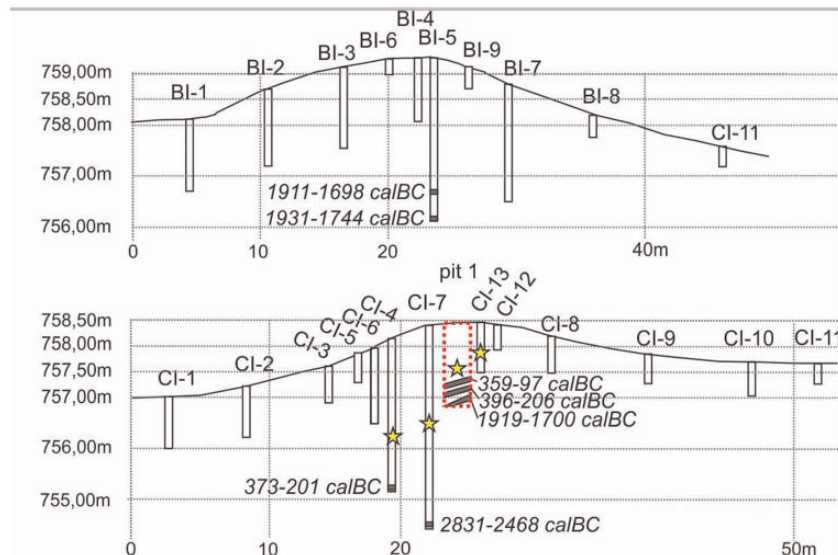
Figure 6. Transects BI and CI (for their location see Figures 3 and 4a), with 'true depth to regolith' for individual corings, location of ^{14}C samples and occurrence of Pompeii tephra layer (indicated with yellow star).
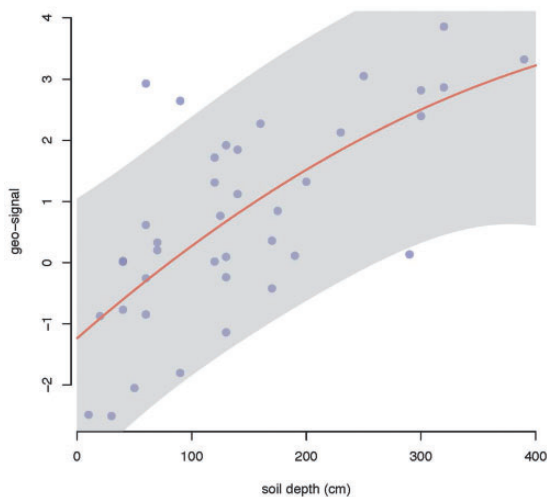
Figure 7. Statistical relation between 'true depth to regolith' and geomagnetic signal for a pixel diameter of 1.0 m. R^2 for the quadratic function (red line) is 0.47; grey area = 90% prediction interval).

Core AE7 holds a prominent Pompeii tephra layer at 110–120 cm depth in a buried A horizon, but has no deeper distinct buried A horizons, suggesting that only one uninterrupted phase of accumulation occurred before the Pompeii eruption event. In the lower part of the coring, bone fragments are common and several large ceramic fragments (impasto, see section 'Dating: [14]C ages, ceramics and tephra') were found. Samples 2–8 are free of tephra and fresh rock is encountered at 320 cm depth.

In core CI7, the Pompeii tephra layer was found at 170–190 cm depth, also in a distinct and thick A horizon. Below this layer, at least one deeper A horizon was encountered. In the deeper layers, ceramic fragments and bone are rare to absent, as well as tephra, but charcoal is present to 400 cm depth, directly above fresh rock, which is at 400 cm.

The fraction >63 um is quite variable in texture and also in composition.

Core CI4 holds tephra throughout. However, between 140 and 150 cm, this is the true Pompeii tephra layer, whereas below (160 cm and deeper) it is tephra in the form of single mineral grains (augite, sanidine, etc.) and pumice fragments in varying quantities. Remarkable is the occurrence at 300–310 cm depth of two perfectly preserved ribs of a small bird, just above the regolith.

Core DG3 holds large amounts of fragments of ceramics, charcoal and bone, as well as fair amounts of limestone fragments. It contains tephra throughout, which is not surprising considering the identification of a ceramic fragment as part of a Roman bowl, and therefore most probably is Pompeii tephra.

Core 20404 is the early core (2013) from which the charcoal provided the ^{14}C datings, on which the identification of the tephra layer as Pompeii tephra from the Somma-Vesuvius was based (see also Sevink et al., 2016 and De Neef, 2016). This coring is situated very close to the later pit 1 (Figure 3). Reference is made to Table 3 and to De Neef (2016) for details, who already extensively described pit 1. Relevant in this context are the ^{14}C datings of the deeper layers encountered (see below).

Dating: 14C ages, ceramics and tephra

Calibrated radiocarbon ages of samples from the various corings and pit 1 are presented in Table 3. The earliest dating is from the base of the fill in coring CI-7 (2831–2468 cal. BC) and falls in the late-Chalcolithic (Ippolito, 2016). The latest is from the upper part of coring 020404-2 and falls in the Imperial Roman period (87–324 cal. AD).

The radiocarbon datings are consistent with the pottery dates. The pottery fragments found on the surface and in pits 1 and 2 consist of handmade pre- or protohistoric pottery made from coarse raw materials known as 'impasto' (e.g. Cannavò et al., 2017) and common wheel-turned coarse wares dating to the Hellenistic and Roman periods (ca. 3rd century BC–4th century AD). The impasto pottery

Table 1. Descriptions of pits 1 and 2.

US/fill phase	Description/fauna/pottery chronology + fabrics	^{14}C age cal. BC
Pit 1		
1	Topsoil, silty clay, brown; small angular stones, charcoal	
	Roman, 2nd–3rd century AD: Common coarse wares incl. African Red Slip Ware (ARSW); Hayes type 197	
2	Silty clay; heterogeneous brown	
3/5	Very dark greyish brown; small stones, charcoal	
	Common coarse wares; incl. ARSW Hayes type 8A: Hellenistic–Imperial Roman (3rd century BC–3rd century AD)	
4/5	Dark yellowish brown, small stones, small charcoal fragments	
	Mandible of large deer; femur epiphysis of cattle; vertebrae of large mammal; unidentified limb bone of large mammal	
	Common coarse wares; coarse impasto; burnt hut loam: EBA; Roman (Imperial)	
5/4	Very dark greyish brown; charcoal, biotite, pumice, small stones	
	Unidentified limb bone of large mammal, complete helicidae land snail shell	
	Common coarse wares; stone: Roman (Imperial)	
6/4	Tephra, light grey. Pompeii eruption 79 AD	
7/4	Small lens, dark greyish brown; biotite, ash, small angular stones	
8/4	Very dark greyish brown; small angular stones, pumice, charcoal	
	Unidentified bone fragments of large mammal; tibia shaft fragment of large mammal	
	Coarse impasto pottery; EBA-MBA1	
9/4	Brown-greyish brown, small stones, charcoal	
10/3	Very dark grey, angular large limestone fragments	359–97
11/3	Dark greyish brown, angular large limestone fragments	396–206
	Thoracic vertebra fragment of cattle	
	Coarse impasto fragment: EBA	
12/2	Dark brown – very dark brown, angular large limestone fragments	1919–1700
	Radius shaft fragment of large mammal; unidentified tooth of mammal, unidentified bone fragment of mammal	
	Coarse impasto pottery; broken greybrown flint flake: EBA	
13/2	Brown, angular large limestone fragments	
14	Brown, angular large limestone fragments	
Pit 2		
1	Topsoil, silty clay, dark brown	
	1 tooth	
	Common coarse wares; coarse impasto: EBA-MBA1; Roman Imperial	
2	Light grey, lime concretions and limestone cobbles	
	1 porcine tooth	
	EBA-MBA1	
3	Yellowish brown	
4	Greyish brown, small stones	
	Coarse impasto pottery, fragment of grinding stone: Late/Middle Neolithic-EBA	
5a	Reddish grey, mottled	
	Common coarse wares, coarse impasto pottery: Roman; EBA	
5b	Grey, small and medium-sized stones	
6	Burnt patch in northern half of test pit, black and bright red spots	1625–1530
	Coarse impasto pottery: EBA-MBA1	
7	Dark grey with reddish spots	
8	Brown	
9	Dark greyish brown, angular large limestone fragments	
10	Limestone blocks in section, wall?	1955–1890
	Charcoal	

US refers to strata distinguished (see also Figure 5). Fill phase numbers refer to phases distinguished. For details of fauna, see de Neef (2016), and on pottery, see Ippolito (2016). 14C ages refer to samples from these pits.
ARSW: African red slip ware; EBA: Early Bronze Age; MBA: Middle Bronze Age.

is generally poorly preserved in the area under study and there are only few fragments with diagnostic features that can be used for typological dating. However, the quality of the ceramics (firing, compactness) and the composition of

the pottery matrix (clays, inclusions) can be used for broad periodical dating. We followed the classification of Ippolito (2016) and her expert knowledge to assign non-diagnostic pottery fragments to archaeological phases. In Table 1 the

Table 2. Composition and characteristics of cores and core sections studied in detail, including radiocarbon ages and 87Sr/86Sr isotopic ratios of samples analysed.

Core and sample	Depth in cm	Gravel size (>2 mm)			Other	Typology ceramics	Cal. BC	% in fraction >62 um			Composition gravel			87Sr/86Sr
		Ce	Ch	Far				f sand	c sand	Gravel	sh/ph	limest	sandst	
DG3/1	90–100	Xx	xx	x	A	–		39	32	29	xx	x	x	
DG3/2	100–110	Xxx	xxx	xxx	–	–		31	21	48	x	(x)	(x)	
DG3/3	110–120	X	xxx	xxx	–	–		45	28	27	xxx	(x)	(x)	
DG3/4	120–125	Xx	xx	xx	Tephra (x)	Roman, bowl		37	30	33	xxx	(x)	x	
DG3/5	125–130	X	x	x	Tephra (x)	–		38	31	31	x	xx	(x)	
DG3/6	130–140	X	x	x	Tephra (x)	–		40	29	31	xx	x	x	
BI5/5	210–220	Xx	–	–	Tephra (x)	–		26	35	39	xxx	(x)	(x)	
BI5/6	220–230	–	xxx	–	Tephra (x)	BA?		30	30	40	xxx	(x)	–	
BI5/7	230–240	Xx	xx	x	Tephra (x)	BA		31	31	39	xxx	(x)	(x)	
BI5/8	240–250	Xx	xx	x	Tephra (x)	BA		32	29	39	xx	x	x	
BI5/9	250–260	Xxx	xxx	xxx	Tephra (x)	BA	1911–1698	35	33	32	xxx	x	(x)	
BI5/10	260–270	Xx	xx	x	A	–		32	32	36	xx	x	–	
BI5/11	270–280	Xxx	x	(x)	–	Neo? coarse impasto		33	32	36	xxx	(x)	–	
BI5/12	280–290	(x)	x	(x)	–	–		35	35	31	xxx	(x)	(x)	
BI5/13	290–300	Xx	x	x	–	–		27	31	42	xxx	(x)	x	
BI5/14	300–310	Xxx	xx	xxx	Wood	Neo? coarse impasto	1931–1744	12	10	78	xxx	(x)	x	
BI5/15a	310–320	(x)	x	x	–	–		8	7	85	xxx	(x)	(x)	
AE7/2	250–260	X	x	x	–	–		34	32	34	xxx	–	–	
AE7/3	260–270	X	x	x	–	BA, too thin for Neo		31	33	36	xxx	(x)	(x)	
AE7/4	270–280	Xxx	x	x	–	EBA? engobe		23	26	52	xxx	(x)	–	
AE7/5	280–290	Xxx	x	x	Large ceramics	BA, compact, burnished		32	33	35	xxx	(x)	(x)	
AE7/6	290–300	X	x	x	Large ceramics	BA, compact		29	30	41	xxx	(x)	x	
AE7/7	300–310	X	x	x	–	BA, burnished		25	30	44	xxx	(x)	(x)	
AE7/8	310–320	X	x	xx	–	–	2133–1903	26	25	49	xxx	x	x	
CI7/5	90–100	(x)	(x)	(x)	–	–		15	27	57	xx	x	x	
CI7/12	160–170	(x)	(x)	–	–	–		–	–	–	xx	x	x	0.707811
CI7/13	170–180	–	x	–	Tephra, snails	–		–	–	–	xx	x	x	0.707676
CI7/14	180–190	(x)	x	(x)	Tephra xxx	–		–	–	–	xx	x	x(x)	0.707755
CI7/25	290–300	–	(x)	–	–	–		24	31	45	xx	x	x	
CI7/26	300–310	–	–	(x)	–	–		24	36	39	xx	(x)	(x)	
CI7/27	310–320	–	(x)	(x)	–	–		41	46	13	xxx	x	x	
CI7/28	320–340	–	(x)	–	–	–		37	28	35	xxx	x	x	
CI7/34	390–400	–	(x)	–	–	–	2831–2468	18	18	65	xx	x	x	

Table 2. Continued.

Core and sample	Depth in cm	Gravel size (>2 mm)				Typology ceramics	Cal. BC	% in fraction >62 um			Composition gravel			^{87}Sr/^{86}Sr
		Ce	Ch	Far	Other			f sand	c sand	Gravel	sh/ph	limest	sandst	
CI4/11	110–120	(x)	x	(x)	Glass, tephra (x)	Roman		38	33	29	xx	x	(x)	
CI4/12	120–130	(x)	(x)	(x)	Tephra (x)	–		41	35	24	xxx	(x)	x	
CI4/13	130–140	(x)	(x)	(x)	Tephra (x)	–		34	29	37	xxx	x	(x)	0.707776
CI4/14	140–150	X	x	–	A, tephra xxx	–		–	–	–	–	–	–	
CI4/15	150–160	(x)	(x)	(x)	A, mouse tooth*	–		40	40	20	xx	x(x)	x	
CI4/16	160–170	(x)	(x)	(x)	A, tephra xxx	–		35	39	26	xxx	x	(x)	
CI4/17	170–180	(x)	xx	(x)	Tephra (x)	–		31	35	34	xx	x	x	
CI4/18	180–190	(x)	xx	(x)		–		29	26	45	xxx	x	(x)	
CI4/19	190–200	(x)	(x)	(x)	A, tephra (x)	–		35	30	35	xxx	x	(x)	
CI4/20	200–210	(x)	(x)	–	A, tephra x	–		–	–	–	xx	x	(x)	
CI4/21	210–220	(x)	xx	–	Tephra (x)	–		41	35	24	xx	x	(x)	
CI4/23	230–240	(x)	(x)	(x)	Chert, tephra (x)	–		39	35	26	xx	x	(x)	
CI4/24	240–250	(x)	(x)	(x)	Tephra x	–		29	37	35	xx	x	(x)	
CI4/25	250–260	(x)	xx	–	A, tephra x	–		47	34	19	xxx	(x)	–	
CI4/26	260–270	(x)	xxx	–	Tephra xx	–		–	–	–	xxx	x	x	0.707662
CI4/27	270–280	(x)	xxx	(x)	Tephra xx	–		–	–	–	xxx	x	x	0.707734
CI4/28	280–290	Xx	(x)	(x)	Tephra xx	–		–	–	–	xxx	x	(x)	0.707801
CI4/29	290–300	Xx	xxx	–	Tephra x	–	373–201	29	29	42	xx	x	(x)	
CI4/30	300–310	–	(x)	–	2 ribs**, 1 vertebra***	–		24	22	53	xxx	x	(x)	

Ce: ceramics; Ch: charcoal; Far: faunal remains (mostly bones); xxx: abundant; xx many; x: common; (x): few; f sand: fine sand (<300 μm); c sand: coarse sand (>300 μm). Neo: Neolithic; BA: Bronze Age; EBA: Early Bronze Age. sh/ph: shale/phyllite; limest: limestone; sandst: sandstone.

*Mouse tooth: MI, upper jaw Myodes glareolus.

**ribs: two small bird ribs.

***vertebra: small snake vertebra.

Table 3. Radiocarbon dates.

Year of sampling	Section/ coring	Sample	Depth in cm	Number	Age	d¹³C	Cal. age	Other	Correlation with US
2015	CI-7	34	390–400	GrA-66072	4025 ± 35	–25.09	2831–2468 cal. BC	No tephra	n.r.
	AE-7	8	310–320	GrA-66067	3635 ± 35	–25.40	2133–1903 cal. BC	No tephra	n.r.
	BI-5	9	250–260	GrA-66070	3495 ± 35	–26.54	1911–1698 cal. BC	Tephra	n.r.
	BI-5	15	310–320	GrA-66071	3510 ± 35	–25.75	1931–1744 cal. BC	No tephra	n.r.
	CI-4	29	290–300	GrA-66226	2215 ± 30	–24.28	373–201 cal. BC	Tephra	n.r.
2013	20404	MDH 1	60–70	GrA-57478	1820 ± 35	–27.36	87–324 cal. AD		US3
		MDH 8	130–140	GrA-57480	2015 ± 30	–24.25	95 cal. BC–61 cal. AD		US5
		MDH 9	140–145	GrA-57481	1945 ± 30	–26.00	21–128 cal. AD	Tephra layer	US6
		MDH 10	145–150	GrA-57482	2080 ± 30	–24.60	191–3 cal. BC		US8
		MDH 14	170–180	GrA-57479	1965 ± 30	–25.55	42 cal. BC–115 cal. AD		US9
		MDH 16	190–200	GrA-57483	2260 ± 30	–25.61	397–209 cal. BC		US10/11
2014	Pit 1	US10	120–130	GrA-60720	2160 ± 35	n.a.	359–97 cal. BC		n.r.
		US11	130–140	GrA-60831	2250 ± 35	n.a.	396–206 cal. BC	Bone collagen	n.r.
		US12	150–160	GrA-60835	3500 ± 35	n.a.	1919–1700 cal. BC	Bone collagen	n.r.
	Pit 2	US 6	50–60	GrA-62338	3310 ± 35	n.a.	1682–1505 cal. BC		n.r.
		190 cm	190	GrA-62341	3580 ± 25	n.a	2022–1882 cal. BC		n.r.

n.a.: not available; n.r.: not relevant. 'Correlation with US layer' refers to the correlation of the sample with the US layer in pit 1. All datings are on the charcoal but for samples GrA-60831 and GrA-60835.
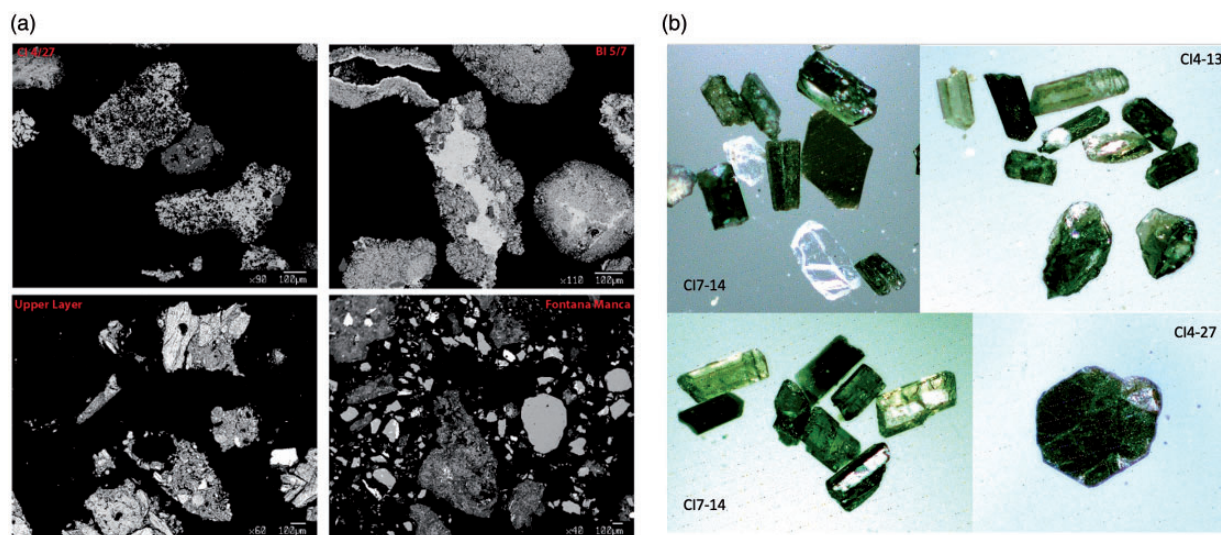

Figure 8. (a) Backscattered (BSE) images of samples selected for electron microprobe analyses. (b) The most abundant mineral phases (pyroxene, feldspar, black mica) in the cored sequences at RB073.

chronological classifications for pottery from pits 1 and 2 are given per stratigraphical unit.

At first instance, thin sections of tephra-containing sediment or pure tephra layers were prepared for microprobe analysis, but none of these held volcanic glass or the rare volcanic glass it contained was weathered. For a next series of thin sections, pumice fragments were selected by hand-picking under the microscope. Their subsequent analysis revealed that these fragments were indeed pumice with abundant mineral fragments (e.g. idiomorphic crystals of feldspar, pyroxenes and the like), but also that the volcanic glass had been completely transformed into amorphous to microcrystalline silica (Figure 8a). In other words, in none of the thin sections we found volcanic glass that was sufficiently fresh to allow for an attribution to a specific eruption on the basis of its elemental chemical composition. Figure 8b shows microphotographs of hand-picked

volcanic minerals encountered, demonstrating the very well-preserved morphology of the idiomorphic pyroxene, feldspar (sanidine) and mica (biotite) crystals, in stark contrast with the complete absence of unaltered volcanic glass.

Sr isotopes were analysed for feldspars collected from in total seven samples, from tephra layers in the CI7 and CI4 cores that based on the ¹⁴C datings were identified as the Pompeii eruption tephra (e.g. CI7/12, CI7/13, CI7/14, CI4/14), and from underlying layers containing volcanic minerals in the same corings (see Table 2). Aliquots of feldspar crystals were hand-picked under a binocular microscope. Samples from CI7 (Pompeii eruption) were found to have an $^{87}Sr/^{86}Sr$ ratio ranging from 0.70768 to 0.70781. Feldspar from CI4 (the upper one from the Pompeii eruption and the lower three from an earlier eruption) are characterized by Sr isotope compositions ranging from 0.70766 to 0.70780. The results are presented in Figure 9, together
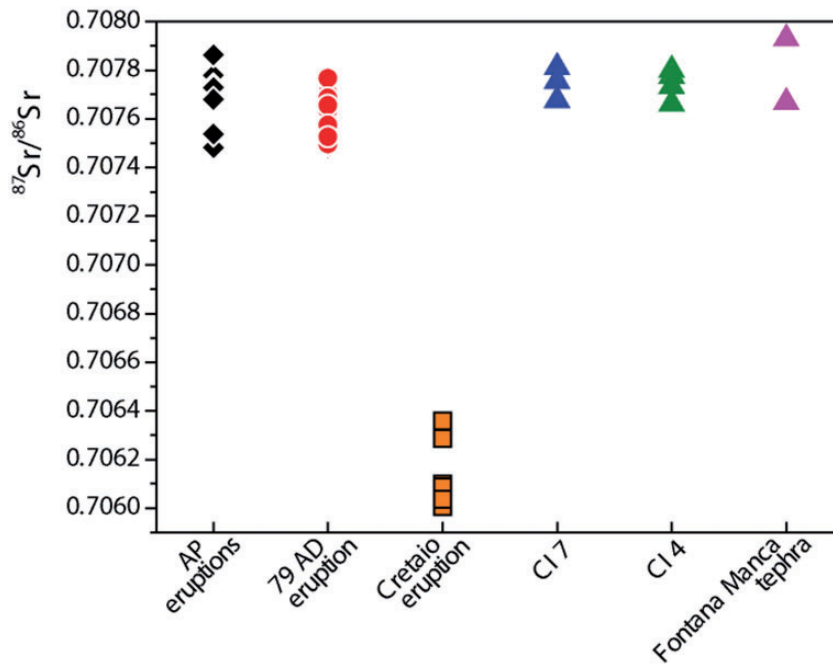
Figure 9. 87Sr/86Sr ratios for tephra from the Pompeii (Civetta et al., 1991) and AP eruptions (Arienzo unpublished data), for feldspars from cores CI-4 and CI-7, and for feldspars and pyroxenes from Fontana Manca (Sevink et al., 2019). The isotope composition of glass from the Cretaio eruption (150 AD Ischia Island, De Vita et al., 2010) has also been reported for comparison.

with the Sr isotope ratios of minerals from the tephra layer at Fontana Manca (Sevink et al., 2019), unpublished data from the AP erupted products and literature data from the Pompeii volcanics (Civetta et al., 1991). Data on the Cretaio eruption (Ischia), which is an explosive eruption that occurred at Ischia in the 2nd century BC, are added for comparison. We refrained from adding Sr-isotopic ratios for late-Pleistocene and Holocene tephra from the Etna (including the FL-tephra), since these are lower than 0.704 (Correale et al., 2014; Corsaro and Pompilio, 2004) and thus decisively exclude an Etnaean origin of our tephra.

Discussion

Morphology of the regolith surface

The regolith surface as based on the observed statistical relation (see Figure 4b) shows a branching somewhat gully like system, with in-between zones with regolith at relatively shallow depth. This system runs more or less perpendicular to the contour lines and across the protruding hillock. The modelled surface also points to the presence of deep pit-like depressions, more or less associated with this system as well as in isolated positions. A typical example is the pit in which core DG3 is located. The reliability of this model is not optimal because of the relatively poor statistical relation found for lesser values of 'depth to regolith' (see Figure 7). Nevertheless, the similarity of the cross sections based on the actual corings and the modelled surface is evident (see Figures 4b and 6).

An explanation for this relatively poor statistical relation can be found in the combination of the large variability in magnetic properties of the various anthropogenic layers (see Figure 5b), and the inclined stratification as observed in that pit. The rapid succession of outcropping layers in pit 1 is exemplary and indicative for the spatial variability in

the composition of the layers encountered below the current plough layer. The overall signals produced by thicker complexes of stacked layers with the same variation in magnetic properties will be less variable, since differences in 'mean signal value' will decline upon increasing thickness of a complex. This most probably explains the far lesser variation in signal value for thicker fills, whereas the heterogeneity in magnetic susceptibility of the anthropogenic material will particularly show up when the depth to regolith is less.

Dense, more or less calcareous fine-grained sedimentary rocks are by far the dominant rock type and results from the corings evidence that rock types with deviating magnetic susceptibility, such as iron-rich sandstones or similar iron-bearing rocks, do not occur. Available data on the magnetic properties of the rock types encountered lead to the conclusion that rock type has at most a very minor effect on the signal compared with the materials that occur in the fill. In other words, the pattern observed must be attributed to the fill characteristics.

In conclusion, the modelled regolith surface is considered to be realistic, at least for its general traits, and for its details that might easily be checked by control corings, aiming at the identification of small pit-like phenomena. The results furthermore evidence that the earlier assumption of a truly mound-like nature of the site (see Sevink et al., 2016) was not correct and was based on insufficient coring data. Nevertheless, even in the highest part of the protruding hillock the in-situ materials (soil/regolith/rock) are covered by a fairly thick anthropogenic layer (see Figures 4b and 6) and 'allochtonic' coarse limestone fragments are encountered at the surface, further evidencing that its surface has been raised. Finally, the whole situation might even be described as a relief inversion, with the originally lowest parts today forming the highest parts of the hillock (see Figure 6).
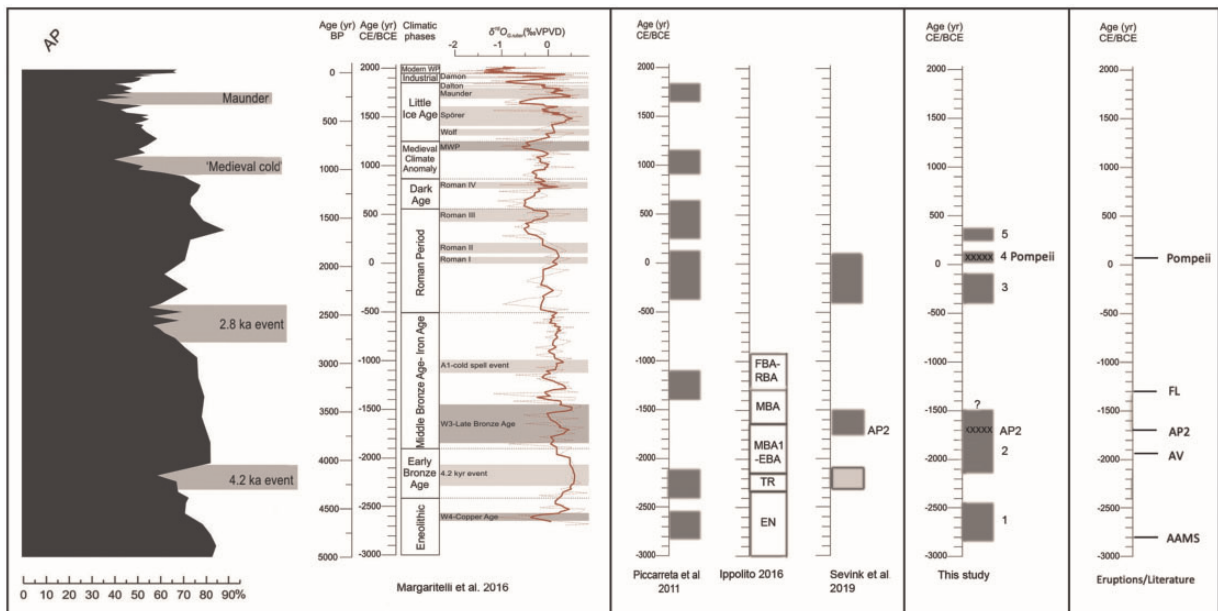
Tephra

In Figure 9, the range of Sr isotope compositions of products erupted during the AP and the Pompeii eruptions has been plotted together with the data for the San Lorenzo samples (site RB073) and Fontana Manca (Sevink et al., 2019). This figure shows that the latter values clearly overlap the range of the AP and Pompeii whole rocks. Additional chemical data for volcanic glass in the tephra layers identified in the cores and pits studied could not be obtained. During the time span in between the Pompeii and AP eruptions the volcanism of the Island of Ischia was also active, with basically low-magnitude eruptions, except for the relatively large-size Cretaio eruption (De Vita et al., 2010) that took place in Roman times. The tephra of this eruption is distributed towards the southeast. To explore all possible correlations, we have also evaluated whether the upper tephra might be attributed to the Cretaio eruption, but the isotopic composition of its tephra (Slejko et al., 2004, unpublished data by Arienzo) differs clearly from our analysed tephra (Figure 9), being much less enriched in radiogenic Sr. For similar reason (see also section 'Dating: ^{14}C ages, ceramics and tephra') an Etnaean origin of our distal tephra could be completely ruled out. Thus, taking also into account the ^{14}C datings (Table 3), there remains no doubt about the source of our distal tephra: the Somma-Vesuvius.

Until very recently, tephra from the Pompeii eruption had not been described for Calabria, which is somewhat surprising considering the thickness of the tephra layer encountered at site RB073, whose origin was earlier established by Sevink et al. (2016) based on ^{14}C datings. Its

thickness is such that it may have had a serious impact on the coeval environment, since tephra holds toxic elements and is physically harmful to humans and animals (see, for example, Blong, 2013; Payne and Egan, 2019; Riede, 2019). An explanation for the low number of recorded occurrences might be that the tephra consists of very loose and easily erodible fine material and, if reworked, may not be recognized without microscopic analysis, similar to the earlier tephra (AP2) at site RB073. As demonstrated by our study, it may also not be readily identified by its chemical composition, chances for finding suited glass shards being very low.

AP2 tephra has been found as a thin layer of juvenile tephra at the nearby site of Fontana Manca, in the Monte Sparviere area, northern Calabria (see Sevink et al., 2019). The Sr-isotopic composition of feldspar and pyroxene from that site is similar to that of the feldspars from the upper and lower tephra-containing samples from the San Lorenzo Bellizzi cores (Figure 9). The same holds for the suite of minerals found as idiomorphic crystals and its pumice content, which is low. Remarkably, for the Fontana Manca tephra layer, similarly to the San Lorenzo Bellizzi tephra, it was impossible to determine its major elements content by electron microprobe: at both sites, glass shards were found to consist of only silica (Figure 8a).

In core BI5, the transition from tephra-free fill to tephra-containing fill has been dated as later than 1931–1744 cal. BC, but earlier than 1911–1698 cal. BC. Since we cannot rule out that some reworking occurred of the charcoal that we dated, these ages should be seen as a *terminus post quem*. Furthermore, the typological

Figure 10. Left: curves by Margaritelli et al. (2016). Centre: phases of instability according to Piccarreta et al. (2011), archaeological periods in Calabria according to Ippolito (2016). Right: results from this study: occupational phases and tephra (AP2, Pompei). Far right: Known relevant eruptions.
AP: arboreal pollen; EN: Eneolithic; TR: transition from Eneolithic to Early Bronze Age; MBA: Middle Bronze Age; EBA: Early Bronze Age; RBA: Recent (late) Bronze age; FBW: Final (late) Bronze Age), results for Lago Forano/Fontana Manca: occupational phases with numbers, tephra (AP2), and 4.2 climatic event, according to Sevink et al. (2019); xxxxx: tephra layer. FL: Etna, Sicani event (Zanchetta et al., 2019); AP2: Somma-Vesuvius eruption (Passareillo et al., 2009; Jung, 2017; Di Vito et al., 2019; Sevink et al., 2019); AV: Somma-Vesuvius Avellino pumice eruption (Zanchetta et al., 2019); AAMS: Campo Flegrei, Agnano-Mt Spina eruptions (Zanchetta et al., 2019).

dating of the ceramics suggests that the tephra was deposited somewhere during the earlier part of the Bronze Age, and thus not seriously later than ca. 1700 cal. BC (see Ippolito, 2016 and Figure 10). This is very much in line with the results for the Fontana Manca tephra layer (around 1700 cal. BC) and those of Jung (2017), who found an age of 1689 ± 24 cal. BC for the AP2 eruption. We can also decisively conclude that the lower tephra in the fill at site RB073 did not originate from the Somma-Vesuvius Avellino eruption. That eruption dates from the Early Bronze Age or, in radiocarbon years, from c. 1900 cal. yr BC and probably even slightly earlier (Alessandri, 2019; Sevink et al., 2011).

Our results thus point to a fairly wide distribution of the AP2 tephra over Southern Italy and highlight its use as a stratigraphic marker for the earlier part of the Bronze Age in this area.

Age of the anthropogenic layers: Tephra, 14C dating, ceramics and phases

The presence of successive A horizons in the thicker fill testifies that phases of landscape and slope stability alternated with phases in which the gully like system was filled in. In principle, these phases in the fill can be dated on the basis of the presence of tephra, ^{14}C datings and typology-based dating of the ceramic fragments. However, their use is constrained by limitations, which are elucidated below. The fills of the smaller depressions, in which phases are harder to establish and distinct A horizons and tephra layers were rarely encountered, cannot be readily attributed to one of the phases. The same holds for the 'pit-like' structures visible in the 3-D bedrock model. Evidently, the thinner surficial 'anthropogenic layer' encountered outside the depressions and pits (see e.g. Figure 4b) is very hard to date, given that it generally lacks stratification, which may well be attributed to deep ploughing in recent times. Nevertheless, its origin is evident from the common presence of 'allochtonic' rock fragments, fragments of ceramics, bone fragments and charcoal.

Tephra. The 79 AD eruption of the Somma-Vesuvius (Pompeii eruption) led to the deposition of a thick tephra layer (3–5 cm), encountered as in situ layer in several corings in the deep central depression and in pit 1. Since this tephra was deposited all over the landscape and in such quantities that any material, eroded or taken from the tephra-covered soil, must hold a significant amount of reworked tephra, it provides a potential *terminus post quem* for the age of that material. Tephra from the AP2 Vesuvian eruption was deposited in distinctly smaller quantity, as can be concluded from its limited thickness (1.5 cm) in the Fontana Manca corings, less than 10 km from this site RB073 (Sevink et al., 2019), where it occurs as an intercalation in a peat section. At our site, it was only encountered as reworked tephra, but nevertheless showed up as a distinct component.

The composition of the Pompeii tephra differs from the AP2 tephra (e.g. Santacroce et al., 2008), potentially allowing for their identification. Unfortunately, in our more or less reworked tephra, fresh glass shards were absent, for which reason we were unable to distinguish between these tephras, either by using the chemical composition of the glass shards or by using the isotope composition of the volcanic minerals (volcanic deposits from AP2 and Pompeii have similar ^{87}Sr/^{86}Sr ratios). Direct and undisputed identification of tephra as AP2 tephra is therefore only possible if an in situ Pompeii tephra layer is present in the sequence above, such as in core BI5 and in pit 1, and in such situations this earlier tephra could be used as an age marker. Evidently, distinction is also possible on the basis of radiocarbon dates or archaeological contexts that testify to a pre-Pompeii age of the tephra concerned.

Finally, it should be emphasized that the in-situ Pompeii tephra layer allows for an extremely precise dating of the surface it covers, as well as of the immediately overlying stratum. Figures 5a and 6 show that this layer occurs on an inclined slope (20–30°), which extends further west (see description of coring 020404, where the same layer is at 140–145 depth). The Pompeii eruption took place in the autumn of 79 AD. Its tephra is encountered as a layer of completely loose and non-cemented silt to fine sand-size tephra. If exposed to subsequent seasonal rains, this tephra would have been easily eroded from the slopes (see e.g. Collins et al., 1983; Sulpizio et al., 2006), implying that it must have been rapidly buried underneath a next layer of anthropogenic material. This material cannot be colluvial in nature (e.g. transported by water), since it is impossible that such colluviation did not touch and largely remove the loose tephra layer. A tentative explanation is that shortly after the deposition of this tephra, 'waste' was dumped on the slope, covering and thus protecting the tephra.

^{14}C dating. The datings were performed on charcoals and collagen extracted from bones, sampled from the fill. Both charcoal and bones may originate from older sources present on the land surface above the depression, being reworked to become part of the fill. The phenomenon is particularly evident when looking at the results for coring 020404, where the Pompeii tephra layer represents an extremely precise and reliable age marker (see Table 3). Evidently, charcoal from the A horizon immediately above the tephra layer (130–140 cm) stems at least partly from a somewhat older charcoal-holding source, resulting in a slight age reversal. A similar slight reversal is seen in the layers below the tephra layer, where the layer from 145 to 150 cm probably also contains some reworked older charcoal. From the above, it is clear that ^{14}C ages obtained need to be interpreted with care and preferably are to be used in combination with other data, that is, on ceramics and tephra. However, they provide evidence on the age of human impacts, particularly for materials containing large amounts of charcoal and serve as a *terminus post quem*.

Ceramics. Precise chrono-typological dating the often small-sized fragments from the coring samples is problematic or even impossible, but Roman and later ceramics can often be identified as such and a broad characterization was feasible, aiding in dating the various layers. Earliest ceramics probably date back to the Neolithic because of their fabric characteristics and were encountered in the deepest layers. Here too, materials may originate from older sources redeposited in the fill as, for example, demonstrated by the combined occurrence of Roman and Protohistoric material in the layers US1-US5 of pit 1, above the Pompeii tephra layer (De Neef, 2016; Table 1). Similar to the ^{14}C datings, the ceramics provide more

general evidence for the human occupation of the area and serve as a *terminus post quem*.

Phases. The gully like system evidently predates the earliest fill, which thus constitutes a *terminus ante quem* for its formation. As for the age of this earliest fill (Complex 1), coring CI-7 is most informative. The lower part of the fill contains charcoal dating back to 2831–2468 cal. BC (Chalcolithic). Ceramics encountered are from the Early Bronze Age or earlier ('impasto'), and this lower fill incidentally contains worked flint. Moreover, charcoal and ceramics are abundant, suggesting that both are coeval with the fill itself and not derived from a significantly older source uphill. Finally, this rather large early fill (see Table 2) is free of tephra and thus predates the AP2 eruption. Archaeologically, this first phase of the fill thus most probably predates the Bronze Age and is of Late Neolithic/Chalcolithic Age (see Alessandri, 2019). Human presence in the upper Raganello Basin is confirmed for these periods, albeit scarcely, and concentrates on the Timpa Sant'Angelo limestone debris cone. Neolithic and Chalcolithic artefacts are reported from sites RB121 and RB214 (De Neef, 2016; Ippolito, 2016). The nearby cave Pietra Sant'Angelo IV contains a Chalcolithic burial. In the Maddalena area, however, this period was not reported until now.

A next early fill (Complex 2) is described by de Neef for pit 1 (see Figure 3 and Table 1) and comprises the combination of US12 (A horizon) and US13, containing angular large limestone fragments. Charcoal in its A horizon produced a date, which is virtually identical to the dates for lower fill material in cores BI-5 and AE-7, and for pit 2, which all are in the same range. Most relevant is core BI-5, since in this core the material immediately above the A horizon holds abundant charcoal, ceramic and bone fragments, which considering their abundance are very unlikely to originate from an earlier source upslope. Moreover, in contrast to the underlying sediment complex (below 260 cm depth) it holds tephra, while this is absent below. Evidently, the onset of Complex 2 predates the AP2 eruption, but will not be significantly older, the ceramics being dated to the Early Bronze Age on the basis of their fabric characteristics.

The upper age limit for this Complex 2 is uncertain. In core BI-5 the A horizon does not contain tephra, but the data from the corings do not point to a major hiatus in the accumulation of material after the deposition of AP2 tephra. On the contrary, this accumulation continued (see e.g. [14]C dating of BI5/9, Table 2). Evidently, whether a true hiatus exists or not is very hard to establish from the available data and it is very well possible that accumulation continued well into the Middle Bronze Age.

The next fill phase (Complex 3) comprises the layers US10 and 11 in pit 1, which are marked by the abundant occurrence of angular large limestone fragments. These fragments are allochtonic, that is, do not occur as bedrock in the area concerned. In this complex, ceramic fragments are rare. The ^{14}C datings, of which the dating on bone collagen is probably the most reliable indicator for the age of this phase, suggest that it dates from the Hellenistic period, between about 400 and 100 BC, as also suggested by the rare ceramics. Although harder to distinguish as a separate phase in the corings, the dating for the corresponding layer in core 20404 is virtually identical to that of pit 1, and the same holds for the thick sequence below the Pompeii tephra layer (at 140–150 cm) in core CI-4. In that core, the [14]C

dating on the charcoal, which together with ceramics is abundantly present immediately above the bedrock, presumably is close to the true onset of this deposit. In this core, it is over 1 m thick (190–310 cm). Remarkably, it contains tephra throughout, suggesting that it consists of material derived from earlier materials that held significant amounts of AP2 tephra.

Complex 4 holds the Pompeii tephra layer and comprises the layers US5-9 in pit 1. The same sequence is observed in all corings holding the tephra layer: intercalated in a thick dark A horizon, with a lighter coloured layer below. A typical example is core CI-4, where the Pompeii tephra layer is also intercalated in a thick A horizon. The dating of this complex as early Imperial Roman is fundamentally based on the age of the tephra layer and is confirmed by the ceramics found in pit 1 (see De Neef, 2016).

Complex 5 is identified in pit 1 and comprises the layers US3-4. In core CI-4 it is evidenced by an A horizon, containing charcoal and ceramics at 100–110 cm depth, separated from the underlying Complex 4 by a 'clean' layer from 120 to 140 cm. A similar situation is encountered in core CI-7. Elsewhere, it may occur immediately below the Ap horizon, since this Ap horizon is often exceptionally thick and at this greater depth regularly contains ceramic fragments. The latest date for the ceramics encountered is the 3rd century AD, suggesting that the A horizon dates from that period or later.

As stated, in the shallower depressions and pits well-identifiable series of phases are far less common and the age of the fill cannot be identified without further detailed research. A typical example is the pit with coring DG-3. The corings showed that the very sharply delineated pit (see Figure 4) had nearly vertical walls and was up to 1.5 m deep, while around this pit bedrock occurred at less than 50 cm depth. The pit was filled with a mixture of soil material and abundant fragments of ceramics, charcoal and bones. A ceramic fragment was identified as a bowl fragment from the Roman period, and the lower part of the fill contained reworked tephra. In sum, the observations suggest that the fill is an intentional dump of waste in a pit dug into the marls, during the post-Pompeii Imperial Roman period. Evidently, similar detailed research is needed to assess the characteristics and origin of the other depression and pits.

Gully like system and fill: Genesis

As already discussed before, the deep gully like system must already have existed before the Late Neolithic and thus originated in a period in which human impacts on the vegetation and landscape were still very limited or even inexistent. The latter can be concluded from palaeoecological studies of relevant nearby sites, which are Lago Trifoglietti (Joannin et al., 2012) and the very nearby Lago Forano and Fontana Manca (Sevink et al., 2019). It is, furthermore, in accordance with the archaeological record for this part of Italy. Most archaeological sites known from this period are situated in the lowlands, such as the Neolithic village of Favella (Tiné, 2009), or in caves (e.g. the cave at Saracena; Tiné and Natali, 2004). Although the archaeological record is still biased in favour of the lower altitudes, human presence in the uplands in this period appears to have been ephemeral and possibly related to seasonal activities rather than permanent habitation.

During the Holocene, under closed natural vegetation and with fine-grained clastic bedrock and dense clayey soils, significant fluvial incision was very unlikely to occur and to result in a deep complex gully like system with steep slopes. In addition, we found no indication for the existence of streams or springs that might have fed such streams. Another indication is the absence of sorted, presumably fluvial materials at the base of the fill that we noted in all corings in this system. The only coring where we found presumably fluvial, well-sorted sediment, was in coring LM-3, situated in the lower section of the depression to the W, but even here it formed part of a younger fill phase, did not occur at the base and was a thin layer only.

During the colder phases of the Late Glacial, full periglacial conditions existed in higher parts of the area, as testified by the presence of a small nivation hollow at ca. 1530 m a.s.l. in the adjacent Mt Sparviere range (Lago Forano, see Sevink et al., 2019). More or less periglacial conditions extended to lower altitudes (see e.g. De Beaulieu et al., 2017), inclusive of the site studied, which is at 750 m a.s.l., and in the unstable marls and shales may have induced mass movements, creating the branched gully like system. We did not find decisive evidence for such origin and thus can only give a tentative explanation for its genesis. Nevertheless, we consider the assumption that the late Neolithic people encountered a dry valley system that only incidentally may have carried some water, as fully warranted.

As for the genesis of the fill complexes, striking is the combination of complete absence of sorting, frequent presence of angular gravel to boulder-size 'allochtonic' limestone fragments, in some instances quite large quantities of ceramic fragments and charcoal, and the abundance of animal bones. In some cases, the latter are exceptionally well preserved, such as the snake vertebra and the small bird's ribs encountered at the base of the Complex 4 fill in core CI-4. The preservation of these fragile bones points to rapid burial upon death and against their prolonged residence in a clayey topsoil. Similar conclusions were drawn regarding the often exceptionally good conservation of the Pompeii tephra layer.

In view of these characteristics, it is concluded that the fill complexes must largely consist of material that was dumped into the gully like incisions and for a large part is 'waste'. Transport by natural processes, such as by overland flow during rainfall events and soil creep or slump, can be excluded as main process, responsible for the genesis of the fill complexes, because of the characteristics mentioned, among which in particular the occurrence of the allochtonic large limestone fragments and complete absence of sorting. An even stronger argument against such 'natural cause' is the observed relief inversion (see above and Figure 6). Whether the material was intentionally dumped to fill the depressions or just dumped as 'waste' could evidently not be established.

Some further indication for the origin of the fill can be found in the quantities of anthropogenic material, encountered as fill. Based on its dimensions, the total volume can be estimated as in the order of 1000 m³. When spread over the overlying slopes and flat ridges, this would yield a layer of the order of 50 cm. However, these slopes and flat ridges are covered by a mantle of anthropogenic material and bear no evidence at all for a massive truncation of their soils. In other words, strong indications exist for a largely allochtonic origin of the fill material, such as debris of huts, houses and other constructions, and household and farm waste, brought into the site from further away. Indications for the origin of the 'fill' are also given by the data on the ceramics and animal remains (see Table 1). These data show that the individual horizons have a rather chaotic composition in terms of the age of the ceramics encountered as based on their typology. Often, within one stratum fragments belonging to entirely different periods are encountered. Furthermore, the incidentally high amount of bone fragments, in the absence of plant macro remains (these were hardly encountered), is striking and points against waste from a regular permanent settlement. Equally remarkable is the large variation in composition of the material as demonstrated by the data in Table 2, which also points to a large temporal variation in its provenance. Together, these observations might suggest that the waste is to be attributed to specific functions through time, including ceremonial (see e.g. the site of Strerro in western Sicily, Leighton, 1998). To fully assess the nature of the fill, evidently a full-scale excavation is needed.

The exact origin of the dark A horizons remains uncertain. They clearly reflect stand-still phases, but whether they are true A horizons, that is, being marked by surficial accumulation of soil organic matter formed by decomposition of litter, is not clear, since its dark colour might also be because of a relatively high content of finely divided charcoal. The fairly neutral term 'occupation horizon' is probably the best description for these horizons, which require more detailed analyses for a proper assessment of their genesis.

Correlation of phases with relevant archaeological, vegetational and palaeoclimatic records

The phases encountered in pits 1 and 2, and in the corings contribute significantly to our understanding of early human occupation of the Raganello uplands. While most protohistoric surface sites recorded by the RAP surveys in the Raganello uplands were dated by Ippolito (2016) to the Middle Bronze Age, our study of site RB073 increases the time depth of human presence by centuries. This also holds for the recent study on the palaeoecology of the upland zone in which the Contrada Maddalena is located (Sevink et al., 2019). In that study, two forest decline phases had been distinguished which date to the Early Bronze Age (around the 4.2 kyr event) and the Middle Bronze Age, respectively, plus a phase of major degradation dated to the Roman period. No indications were found for an earlier – pre-Early Bronze Age – significant anthropogenic impact.

The lowest level of RB073 (CI-7-34) predates the first phase of forest decline related to the 4.2 kyr event by several centuries and although pottery from this period appears absent in the cores and in pit 1, pit 2 did yield ceramics from the Chalcolithic period. This is in accordance with the Chalcolithic date of the burial in the Pietra Sant'Angelo IV cave (Larocca et al., 2019), thus indicating ephemeral human presence in the Raganello uplands at an early stage. The Early Bronze Age–Middle Bronze Age occupational phase (Complex 2) fits the intensification of settlement of the uplands as well as the related human impact on the forests. The lack of Late Bronze Age potsherds (Bronzo Recente and Bronzo Finale, ca. 1350–1000 BC) is also consistent with the general reduction in sites and concentration of settlement in the foothills during this

period (De Neef, 2016; Ippolito, 2016). The Hellenistic materials encountered in pits 1 and 2 are consistent with the contemporary settlement site RB174. Roman occupation of the uplands is so far only thinly represented and may be above all related to transhumance routes, as is the case elsewhere in Southern Italy. The Roman degradation phase still needs to be evaluated in the light of possible Roman land use for which, however, insufficient data are available for our study area as of yet.

Evidently, the questions arise whether the observed anthropogenic phases are linked to climatic phases with favourable conditions for human occupation and thus can be seen as a climatic signal, and whether the observed phases also show up in other studies on early land use in Southern Italy (e.g. Mercuri et al., 2011; Roberts et al., 2011).

Detailed mid/late-Holocene palaeorecords for the uplands of mainland Southern Italy are scarce and limited to those for Lago Trifoglietti (De Beaulieu et al., 2017; Joannin et al., 2012) and for Lago Grande di Monticchio (Allen et al., 2002). Di Rita and Magri (2019) reviewed the impact of the 4.2 ka event in the vegetation record of the central Mediterranean and concluded that for both palaeorecords changes in vegetation related to this climatic event are uncertain. Moreover, they stated that for Monticchio 'no vegetation change is unambiguously attributed to human impact' by Allen et al. (2002), though Allen et al. reported that 'the last 2000 years are made distinctive by evidence for forest clearance and agricultural activity'. Furthermore, Di Rita and Magri cited that 'at Trifoglietti only poor imprints of agricultural activity and anthropogenic indicators are visible in the record and that the strongest evidence of human impact is considered the selective exploitation of fir, especially after 4 ka'.

Piccarreta et al. (2011) came to quite different conclusions, partly based on the same record (Monticchio), for the nearby but lower Basilicata. They concluded that repeated phases of increased fluvial activity are probably climatically driven (see also Figure 10), implying a far more variable climatic record than described by Di Rita and Magri (2019). Furthermore, they stated that 'it is in the last 2000 years that human impact forces enhanced geomorphic activity'. Unfortunately, there are serious doubts about their dating of the early phases, since they state that 'shortly before 4300 cal years BP 10 to 50 cm-thick "Avellino" tephra layers were deposited' and use those datings in their chronology. Currently, it is widely agreed upon that this Avellino eruption dates from ca. 3850 cal. years BP (e.g. Alessandri, 2019; Livadie et al., 2019).

A quite detailed reconstruction of the palaeoclimate and palaeoenvironment for the last 5 millennia was presented by Margaritelli et al. (2016), based on a marine palaeoecological record from the Gulf of Gaeta. Although this is further northwest along the Tyrrhenian coast, they linked the climatic intervals distinguished to archaeological/cultural periods, which allows for a more detailed comparison with our phases and results, including those from the study of the Lago Forano/Fontana Manca cores (Sevink et al., 2019). Remarkably, they found little evidence for early agriculture (e.g. cereal cultivation), which is known to have had a major impact on the Late Neolithic and Bronze Age landscape and vegetation of the Campanian plains (see e.g. Livadie et al., 2019; Vanzetti et al., 2019). This phenomenon is also dealt with in a later paper on this core by De Rita et al.

(2018), who attributed this poor representation to the low dispersal of cereal pollen. The results of Piccarreta et al. (2011) and Margaritelli et al. (2016) are summarized in Figure 10, together with the early archaeological phases distinguished by Ippolito (2016) and the phases that we distinguished (Sevink et al., 2019 and current paper).

Figure 10 illustrates that there is no significant correlation between our phases and the impact phases of Piccarreta et al. (2011), nor the climatic phases distinguished by Margaritelli and Di Rita et al. (2018). There is also no match regarding the age, magnitude and phasing of anthropogenic impacts with the records for Trifoglietti and Monticchio, which are both from the uplands of Southern Italy. This strongly suggests that for the last ca. 5 millennia inland palaeoecological records, even those for Trifoglietti and Monticchio, most probably reflect local to sub-regional scale variations in vegetation and land use history, rather than supra-regional variations, and is fully in line with the explanation given by De Rita et al. (2018) for the marked absence of indicators for human impacts in the Bronze Age section of the Gulf of Gaeta core.

General discussion and conclusion

Based on the small number of more or less accidental finds and results from archaeological field surveys, it was traditionally assumed that the mountainous inlands of Southern Italy were sparsely inhabited during the period spanning the Late Neolithic to the Late Roman period (De Neef et al., 2017). Finds consist of materials encountered in caves and of rare small scatters of artefacts (mostly pottery fragments). This rare occurrence of archaeological remains might be due to a serious bias in the archaeological record as reflected by surface finds, brought about by strong later erosion and, notably, plough erosion in connection with intensive modern land use. Attempts to master such bias gave rise to the development of predictive archaeological models that aim to account for the impact of later natural processes. The Caleros model by Feiken (2014), largely based on a detailed spatial soil erosion model, is an example of such predictive models. It was applied to the Upper Raganello catchment and indicated that at the site studied erosion had a severe impact on the archaeological archive, destroying a significant part of the soil profile in most of the area.

Our study demonstrates one of the serious limitations of such models, which is that they do not account for human activities that do not conform to natural slope processes, such as the dumping of waste materials and the resulting relief reversal that we observed. It is the thorough multidisciplinary approach of field walking, geophysical survey and invasive research that led to the discovery of the major archaeological archive that we describe in this paper. Without such an approach it would have remained unnoticed. Moreover, our study also demonstrates that geophysical surveys, if combined with adequate soil data, can provide much more than a broad picture of topsoil geomagnetic anomalies. Provided that sufficient contrast in geomagnetic properties exists between a fill and the undisturbed soil, we could identify features to a depth of about 4 m. Here too, we show the merits of a thorough multidisciplinary approach, rather than seeing geophysical surveys as a means to broadly survey disturbances and anthropogenic structures in the topsoil.

The multi-phased archaeological archive most probably largely consists of dumped waste with a significant amount of pottery, bone and charcoal fragments. Initially it filled a complex of gully like depressions and pits, but later on turned into a mound-like accumulation of anthropogenic debris with associated relief reversal. This deposit covers a period of about 3 millennia, ranging from Late Neolithic/ Chalcolithic to the Late Imperial Roman Period, and holds tephra from two Somma-Vesuvius eruptions: the AP2 eruption from around 1700 cal. BC and the Pompeii eruption from 79 AD. The earliest phase in the built-up of the archive predates the earliest anthropogenic phase identified in the recent palaeoecological study of Fontana Manca and Lago Forano (Sevink et al., 2019). The next four phases match well with the results of that study and the regional archaeological inventory. This suggests that the sequence of phases of anthropogenic impacts on the vegetation and landscape, in this part of Calabria, is a regional rather than a local phenomenon, and that these impacts escaped their recognition in palaeorecords, thus far established for this region.

Although comparable sites are known from Sicily (Leighton, 1998), because of both its composition and dimensions, the site seems unique for the area concerned and, probably, for the mountainous inland of Southern Italy in general. Whether it had a specific function is not clear, but an answer to that question might be gained through a systematic excavation, which has not yet been performed.

The identification of Somma-Vesuvius distal tephras in northern Calabria provides important constraints for reconstruction of terrestrial sequences in this region. In particular, the 79 AD tephra was found in several cores from the Tyrrhenian and Ionian Sea (e.g. Zanchetta et al., 2011 and references therein), but it has not yet been reported for terrestrial sites in this part of Southern Italy. Furthermore, the tephra of the AP2 eruption, which we identified through detailed study of the archive, has not been reported before, except for its occurrence at Fontana Manca (Sevink et al., 2019) and – as cryptotephra – in a Gulf of Taranto marine core (Di Donato et al., 2019; Insinga et al., 2020). Its distinct presence at both the site RB073 and the Fontana Manca site suggests a considerably more massive eruption in terms of the ejected volume of pyroclastics, than currently assumed (e.g. distributed in a small area around the volcano and 5% of the volume of the Pompeii eruption according to Andronico and Cioni, 2002). Together with the ^{14}C datings, these two tephra falls provide an excellent framework for identifying the various phases and also allow for a very precise and useful correlation among different environments and human settlements in northern Calabria.

We conclude that for the period concerned (ca. last 5 millennia) and at least for the uplands of Southern Italy, clear evidence exists for varied and quite complex temporal and spatial patterns in vegetation and prehistoric land use. Therefore, reliable interpretations of records from this area at national or even supranational scale require a larger and more evenly spread number of palaeorecords than those currently available (Monticchio and Trifoglietti) and a better insight into the link between prehistoric land use as based on regional archaeological surveys and its visibility in palaeoecological records.

Declaration of conflicting interests

The author(s) declared no potential conflicts of interest with respect to the research, authorship and/or publication of this article.

ORCID iD

Jan Sevink https://orcid.org/0000-0002-0147-9821

References

Archaeological evidences are often published in local Italian journals or proceedings. For completeness they are given in the text where relevant, but generally they cannot be digitally retrieved. They are indicated with an *.

Alessandri L (2019) The early and Middle Bronze Age (1/2) in south and central Tyrrhenian Italy and their connections with the Avellino eruption: An overview. *Quaternary International* 499: 161–185.

Allen JRM, Watts WA, McGee E et al. (2002) Holocene environmental variability: The record from Lago Grande di Monticchio, *Italy. Quaternary International* 88(1): 69–80.

Andronico D and Cioni R (2002) Contrasting styles of Mount Vesuvius activity in the period between the Avellino and Pompeii Plinian eruptions, and some implications for assessment of future hazards. *Bulletin of Volcanology* 64(6): 372–391.

Arienzo I, Carandente A, Di Renzo V et al. (2013) Sr and Nd isotope analysis at the Radiogenic Isotope Laboratory of the Istituto Nazionale di Geofisica e Vulcanologia, Sezione di Napoli: Osservatorio

Vesuviano. *Rapporti Tecnici INGV* 260: 1–18. Available at: http://istituto.ingv.it/l-ingv/produzione-scientifica/rapporti-tecnici-ingv/archivio/rapporti-tecnici-2013/

Armstrong K and Van Leusen M (2012) Rural life in protohistoric Italy: Using integrated spatial data to explore protohistoric settlement in the Sibaritide. In: *Proceedings of the 40th conference in computer applications and quantitative methods in archaeology*, Southampton, 26–30 March.

Blong RJ (2013) *Volcanic Hazards: A Sourcebook on the Effects of Eruptions*. Amsterdam: Elsevier.

Boenzi F, Caldara M, Capolongo D et al. (2008) Late Pleistocene-Holocene landscape evolution in Fossa Bradanica, Basilicata (southern Italy). *Geomorphology* 102(3–4): 297–306.

Bronk Ramsey C (2017) OxCal 43. Available at: https://c14.arch.ox.ac.uk/oxcal.html

Cannavò V, Cardarelli A, Lugli S et al. (2017) Fabrics and archaeological facies in northern Italy: An integrated approach to technological and stylistic choices in Bronze Age pottery production. *Journal of Archaeological Science: Reports* 16: 521–531.

Civetta L, Galati R and Santacroce R (1991) Magma mixing and convective compositional layering within the Vesuvius magma chamber. *Bulletin of Volcanology* 53: 287–300.

Collins BD, Dunne T and Lehre AK (1983) Erosion of tephra-covered hillslopes north of Mount St. Helens, Washington: May 1980-May 1981. *Zeitschrift fur: Geomorphologie* 43: 103–121.

Correale A, Paonita A, Martelli M et al. (2014) A two-component mantle source feeding Mt. Etna magmatism: Insights from the geochemistry of primitive magmas. *Lithos* 184: 243–258.

Corsaro RA and Pompilio M (2004) Dynamics of magmas at Mount Etna. *Geophysical Monograph-American Geophysical Union* 143: 91–110.

Crocitti M, Sulpizio R, Insinga DD et al. (2019) On ash dispersal from moderately explosive volcanic eruptions: Examples from Holocene and Late Pleistocene eruptions of Italian volcanoes. *Journal of Volcanology and Geothermal Research* 385: 198–221.

De Beaulieu JL, Brugiapaglia E, Joannin S et al. (2017) Lateglacial-Holocene abrupt vegetation changes at Lago Trifoglietti in Calabria, Southern Italy: The setting of ecosystems in a refugial zone. *Quaternary Science Reviews* 158: 44–57.

De Neef W (2016) *Surface <> subsurface: A methodological study of Metal Age settlement and land use in northern Calabria (Italy)*. PhD Thesis, University of Groningen.

De Neef W, Armstrong K and Van Leusen M (2017) Putting the spotlight on small Metal Age pottery scatters in northern Calabria (Italy). *Journal of Field Archaeology* 42(4): 283–297.

De Neef W, van Leusen M, Armstrong K et al. (2019) Between a rock, a gully, and a hard place: Archaeological prospection of Metal Age remains in the uplands of the Raganello Basin (Calabria, Italy). *Funde in der Landschaft, LVR Amt für Bodendenkmalpflege im Rheinland* 26: 159–169.

De Vita S, Sansivero F, Orsi G et al. (2010) Volcanological and structural evolution of the Ischia resurgent caldera (Italy) over the past 10 ky. *Geological Society America Special Paper* 464: 193–239.

Di Donato V, Insinga DD, Iorio M et al. (2019) The palaeoclimatic and palaeoceanographic history of the Gulf of Taranto (Mediterranean Sea) in the last 15 ky. *Global and Planetary Change* 172: 278–297.

Di Rita F and Magri D (2019) The 4.2 ka event in the vegetation record of the central Mediterranean. *Climate of the Past* 15: 237–251.

Di Rita F, Lirer F, Bonomo S et al. (2018) Late Holocene forest dynamics in the Gulf of Gaeta (central Mediterranean) in relation to NAO variability and human impact. *Quaternary Science Reviews* 179: 137–152.

Di Vito MA, Talamo P, de Vita S et al. (2019) Dynamics and effects of the Vesuvius Pomici di Avellino Plinian eruption and related phenomena on the Bronze Age landscape of Campania region (Southern Italy). *Quaternary International* 499: 231–244.

FAO (2006) *Guidelines for Soil Description*. 4th Edition. Rome: FAO.

Feiken H (2014) Dealing with Biases: Three Geo-Archaeological Approaches to the Hidden Landscapes of Italy, vol. 26. Eelde: Barkhuis.

Ghezzi G (1973) *Carta geologica della Calabria alla scala di 1:25.000: Nota illustrative delle tavolette appartenenti al foglio 222della carta topografica d'Italia dell'I.G.M. (al 1:100.000): Amendolara*. Amendolara: Cassa per opera straordinarie di pubbico interesse nell'Italia meridionale (Cassa per il Mezzogiorno).

Giannini G, Burton AN, Ghezzi G et al. (1963) Carta geologica della Calabria alla scala di 1:25.000. Nota illustrative delle tavolette appartenenti al foglio 221 della carta topografica d'Italia dell'I.G.M. (al 1:100.000): Castrovìllari. Castrovìllari: Cassa per opera straordinarie di pubbico interesse nell'Italia meridionale (Cassa per il Mezzogiorno).

Goldstein SL, Deines P, Oelkers EH et al. (2003) Standards for publication of isotope ratio and chemical data in Chemical Geology. *Chemical Geology* 202: 1–4.

Insinga DD, Petrosino P, Alberico I et al. (2020) The Late Holocene tephra record of the central Mediterranean Sea: Mapping occurrences and new potential isochrons for the 4.4–2.0 ka time interval. *Journal of Quaternary Science* 35(1–2): 213–231.

Ippolito F (2016) *Before the Iron Age: The oldest settlements in the hinterland of* the Sibaritide (Calabria, Italy). PhD Thesis, University of Groningen.

Jahn R, Blume HP, Asio VB et al. (2006) *Guidelines for Soil Description*. Rome: FAO.

Joannin S, Brugia paglia E, Beaulieu JL et al. (2012) Pollen-based reconstruction of Holocene vegetation and climate in southern Italy: The case of Lago Trifoglietti. *Climate of the Past* 8(6): 1973–1996.

Jung R (2017) Chronological problems of the Middle Bronze Age in Southern Italy. In: Lachenal T, Mordant C, Nicolas T et al. (eds) Le Bronze moyen et l'origine du Bronze final en Europe occidentale (XVIIe–XIIIe siècle av. J.-C.). Colloque international de l'APRAB. Strasbourg, 17 au 20 juin 2014. Strasbourg: Mémoires d'Archéologie du Grand-Est, pp. 623–642.

Larocca F, Minelli A and Larocca A (2019) Dentro la Pietra Sant'Angelo: Viaggio alla scoperta della preistoria nelle grotte di San Lorenzo Bellizzi. *Speleologia* 80: 24–31.

Leighton R (1998) *Sicily before History, an Archaeological Survey from the Palaeolithic to the Iron Age*. Ithaca, NY: Cornell University Press.

Livadie CA, Pearce M, Delle Donne M et al. (2019) The effects of the Avellino Pumice eruption on the population of the Early Bronze age Campanian plain (Southern Italy). *Quaternary International* 499: 205–220.

Longin R (1971) New method of collagen extraction for radiocarbon dating. *Nature* 230(5291): 241–242.

Margaritelli G, Vallefuoco M, Di Rita F et al. (2016) Marine response to climate changes during the last five millennia in the central Mediterranean Sea. *Global and Planetary Change* 142: 53–72.

Mercuri AM, Sadori L and Uzquiano Ollero P (2011) Mediterranean and north-African cultural adaptations to mid-Holocene environmental and climatic changes. *The Holocene* 21(1): 189–206.

Passariello I, Livadie CA, Talamo P et al. (2009) 14 C Chronology of Avellino Pumices Eruption and timing of human reoccupation of the devastated region. *Radiocarbon* 51(2): 803–816.

Payne RJ and Egan J (2019) Using palaeoecological techniques to understand the impacts of past volcanic eruptions. *Quaternary International* 499(Part B): 278–289.

Piccarreta M, Caldara M, Capolongo D et al. (2011) Holocene geomorphic activity related to climatic change and human impact in Basilicata, *Southern Italy*. *Geomorphology* 128(3–4): 137–147.

Riede F (2019) Doing palaeo-social volcanology: Developing a framework for systematically investigating the impacts of past volcanic eruptions on human societies using archaeological datasets. *Quaternary International* 499(Part B): 266–277.

Roberts N, Brayshaw D, Kuzucuoğlu C et al. (2011) The mid-Holocene climatic transition in the Mediterranean: Causes and consequences. *The Holocene* 21(1): 3–13.

Santacroce R, Cioni R, Marianelli P et al. (2008) Age and whole rock–glass compositions of proximal pyroclastics from the major explosive eruptions of Somma-Vesuvius: A review as a tool for distal tephrostratigraphy. *Journal of Volcanology and Geothermal Research* 177(1): 1–18.

Sevink J, Bakels CC, Di Vito MA et al. (2019) Holocene vegetation record of upland northern Calabria, Italy: Environmental change and human impact. *The Holocene* 29(4): 633–647.

Sevink J, den Haan M, van Leusen M et al. (2016) *Raganello Basi n Studies 2: Soils and Soil Landscapes of the Raganello River Catchment (Calabria, Italy)*. Eelde: *Barkhuis*; Groningen: Groningen Institute of Archaeology.

Sevink J, van Bergen MJ, van der Plicht J et al. (2011) Robust date for the Bronze age Avellino eruption (Somma-Vesuvius): 3945±10 calBP (1995±10 calBC). *Quaternary Science Reviews* 30(9-10): 1035–1046.

Slejko FF, Petrini R, Orsi G et al. (2004) Water speciation and Sr isotopic exchange during water-melt interaction: A combined NMR-TIMS study on the Cretaio Tephra (Ischia Island, south Italy). *Journal of Volcanology and Geothermal Research* 133(1–4): 311–320.

Sulpizio R, Zanchetta G, Demi F et al. (2006) The Holocene syneruptive volcaniclastic debris flows in the Vesuvian area: Geological data as a guide for hazard assessment. In: Siebe C, Macías JL and Aguirre-Díaz GJ (eds) *Neogene-Quaternary Continental Margin Volcanism: A Perspective from México, vol. 402*. Boulder, CO: Geological Society of America, pp. 203–221.

Tiné V and Natali E (2004) La Grotta San Michele di Saracena (CS): una sequenza stratigrafica dal Neolitico Antico al Bronzo Medio. In: *Atti della XXXVII Riunione Scientifica* di Preistoria e Protostoria IIPP, Firenze, 29 September–4 October.*

Tiné V (ed.) (2009) Favella: un villaggio neolitico nella Sibaritide. Rome: Museo nazionale preistorico etnografico 'L. Pigorini'.*

Van Leusen M and De Neef W (2018) On the trail of pre- and protohistoric activity around San Lorenzo Bellizzi: Geo-archaeological studies of the Groningen Institute of Archaeology, 2010-2015. Il Pollino, barriera naturale e crocevia di culture. Giornate internazionali di archeologia, San Lorenzo Bellizzi, 16-17 Aprile 2016. In: Colelli C and Larocca A (eds) *Cosenza: Ricerche – Collana del Dipartimento di Studi Umanistici, Sezione Archeologia*, vol. 12. Calabria: Università di Calabria, pp. 39–47.*

Van Leusen PM, Kattenberg A and Armstrong K (2014) Magnetic susceptibility detection of small protohistoric sites in the Raganello basin, Calabria (Italy). *Archaeological Prospection* 21(4): 245–253.

Vanzetti A, Marzocchella A and Saccoccio F (2019) The Campanian agrarian systems of the late Copper-Early Bronze Age (ca. 4550-3850 cal BP): A long-lasting agrarian management tradition before the Pomici di Avellino eruption. *Quaternary International* 499: 148–160.

Zanchetta G, Bini M, Di Vito MA et al. (2019) Tephrostratigraphy of paleoclimatic archives in central Mediterranean during the Bronze Age. *Quaternary International* 499: 186–194.

Zanchetta G, Sulpizio R, Roberts N et al. (2011) Tephrostratigraphy, chronology and climatic events of the Mediterranean basin during the Holocene: An overview. *The Holocene* 21(1): 33–52.